University of Nairobi

School of Engineering

DEPARTMENT OF GEOSPATIAL AND SPACE TECHNOLOGY

Monitoring Tree Cover Changes in Kenya's Five Major Water Towers using Geospatial Technologies

BY

Kuto K. Edmond

F56/11770/2018

Report submitted in partial fulfillment of the requirements for the Degree of Master of Science in Geographic Information Systems, in the Department of Geospatial and Space Technology of the University of Nairobi

August 2020

Declaration of originality

Name of student: **Kuto K. Edmond**

Registration: **F56/11770/2018**

College: **Architecture and Engineering**

Faculty/School/Institute: **School of Engineering**

Department: **Geospatial and Space Technology**

Course Name: **Master of Science in Geographic Information Systems**

Title of work: **Monitoring Tree Cover Changes in Kenya's Five Major Water Towers using Geospatial Technologies**

1) I understand what plagiarism is and I'm aware of the university policy in this regard
2) I declare that this research project is my original work and has not been submitted elsewhere for examination, award of a degree or publication. Where other works or my own work has been used, this has properly been acknowledged and referenced in accordance with the University of Nairobi's requirements
3) I have not sought or used the services of any professional agencies to produce this work
4) I have not allowed , and shall not allow anyone to copy my work with the intention of passing it off as his/her work
5) I understand that any false claim in respect of this work shall result in disciplinary action in accordance with University of Nairobi anti-plagiarism policy

Signature:___________________

Date:_______________________

Turn it in report summary

MSc GIS final project report_Kuto_Edmond_turnitin

ORIGINALITY REPORT

4%	6%	3%	4%
SIMILARITY INDEX	INTERNET SOURCES	PUBLICATIONS	STUDENT PAPERS

PRIMARY SOURCES

1	www.fao.org Internet Source	1%
2	wedocs.unep.org Internet Source	1%
3	dspace.ut.ee Internet Source	1%
4	bioone.org Internet Source	1%
5	www.tandfonline.com Internet Source	1%
6	www.kenyaforests.org Internet Source	1%
7	www.absoluteastronomy.com Internet Source	1%

Submission date: 18-Aug-2020 10:37AM (UTC+0300)
Submission ID: 1242998869
File name: Turn_it_in_final_report.docx (12.91M)
Word count: 8449
Character count: 46961

STUDENT:

Kuto K. Edmond: SIGNATURE…………………………….DATE………………..……………..
F56/11770/2018

SUPERVISORS:

Mr. Wakoli Peter C. M.: SIGNATURE…………………………….DATE………………..……………..

ABSTRACT

Water towers are the hearts that pump life into any ecosystem by providing fresh water recharge to sustain most living organisms that facilitate the very existence of humans. Numerous studies have documented the importance of these water towers in sustenance of fresh water that account for only about three percent of the Earth's water. While the role water towers play in ensuring our survival is clear, they are continuously and gradually being degraded as a result of pressure from demographic factors in addition to uncontrollable natural factors. Inadequate information about the area and spatial extents of tree cover loss jeopardizes systematic monitoring of these forests. This has led to haphazard restoration efforts that tend to be unsuccessful in the long term. Earth observation technology enables efficient and effective mapping and monitoring of forest cover within water towers over an extensive range of temporal and spatial scales. This study applied remote sensing techniques to investigate the amount of tree cover lost between 2005 and 2019 in Kenya's major water towers using Landsat 30-m resolution imagery. The images were classified into two classes, tree cover and non-tree cover, from which change detection maps were produced with their underlying statistics of tree cover loss in terms of area and location. The study established a trend in tree cover loss across all the water towers where Mt. Kenya experienced approximately 7% decline, Mt. Elgon 14%, Aberdare range 18%, Mau complex 24% and Cherangani hills 25% which all amount to an average of 19% throughout the study period. The government and NGOs should therefore apply geospatial techniques in monitoring tree cover. This will enable proper identification of degraded areas within forests and further make informed decisions in formulating policies and executing restoration programmes.

Keywords: **Water towers, tree cover, forests, fresh water, Landsat.**

DEDICATION

I would like to dedicate my work to the Almighty God for continuous provision, good health and guidance throughout my research project and to my loving late mom who is not here to witness this great milestone of achievement in my life. I thank my sister and my family at large for the encouragements and support throughout my study.

ACKNOWLEDGEMENTS

Special gratitude to my supervisor Mr. Wakoli Peter C. M. for his constructive criticism, ideas, support and availability throughout my research period to make it a success. My further appreciation goes to the staff of the Geospatial and Space Technology department who have played a significant role in my studies from the time I began my course work and now a successful end.

I would also like to acknowledge Mr. Stephen Kibet for your continuous support, insights and input throughout my course with never ending encouragements and prayers. I pass my sincere gratitude to my classmates for the support received from the time we started the course whom we together made the journey a success.

Table of Contents

List of tables

List of figures

Nomenclature

KWTA- Kenya Water Towers Agency

UNFCCC- United Nations Framework Convention on Climate Change

UNCCD- United Nations Convention to Combat Desertification

UNCBD- United Nations Convention of Biological Diversity

CBD- Convention of biological diversity

ASAL- Arid and Semi-Arid Land

NGO- Non-governmental Organization

MOEF- Ministry of Environment and Forestry

MOEWNR- Ministry of Environment, Water and Natural Resources

UNESCO- United Nations Educational, Scientific and Cultural Organization

LULC- Land Use and Land Cover

ETM+- Enhanced Thematic Mapper Plus

RF- RandomForest

IUCN- International Union for Conservation of Nature

GPFLR- Global Partnership on Forest and Landscape Restoration

WRI- World Resource Institute

SDSU- South Dakota State University

IPCC- Intergovernmental Panel on Climate Change

MRV- Monitoring, Reporting and Verification

1. INTRODUCTION

1.1 Background

Anything concerning water resources, the significant terms "water tower" or "water catchment" have been widely adopted currently to convey the value of mountainous regions in supplying freshwater to vicinal downstream areas (Viviroli et al. 2007). Forested catchments form water towers which engirdle upland areas with characteristics to support reception, infiltration, percolation and storage of rainfall and gradually releases it into a drainage basin (KWTA 2019). These catchments are responsible for providing base flow to rivers, lakes and spring water as well as ground water recharge.

Kenya's Afromontane forests, where most water towers lie, provide both tangible products such as basic livelihood requirements ranging from food, fiber and fodder as well as intangible services that protect local communities from landslides, erosion, strong winds and maintain micro climate to regulate temperature and rainfall for fresh water recharge (Ongugo et al. 2014).

Globally, over two billion individuals presently survive under severe water stress due to poor access to freshwater, a figure expected to hit its double by 2025 (Wallström et al. 2004). This can be directly translated to Kenya's scenario whose 89% of total land is categorized as ASAL (Njoka et al. 2016). As a result, its citizens' access to freshwater is under threat, whose impact will increase with current trends in adverse climate change.

Many issues arise when it comes to forest restoration. An analysis conducted by IUCN, GPFLR, WRI and SDSU in the year 2011 discovered that over 2 billion hectares of land could benefit from restoration globally but where the restoration efforts should be focused is an issue(Bainbridge 2017). Lack of political good will has seen such efforts jeopardized, which is subject to change depending on the incumbent government's stance on such matters (Zarembka n.d.). In matters tree planting, location is vital for tree survival where it has been noted that there can be success in existing forest preservation rather than trying to create one where there wasn't any before (Geiling n.d.). Base information, which is presently scanty, is required to direct restoration efforts and thus efficiently select restoration areas.

Accurate and consistent land-cover change estimates yield a basis for comprehending the prospective effects of changes on the ecosystem and the services they provide (Krylov et al. 2018). Such estimates are a vital component of national and local resource management and mechanisms for reporting techniques, such as those commitments outlined in international agreements like the UNFCC, UNCCD and UNCBD (Horowitz 2016; UNCCD 2014; UNCBD 1996).

Tree cover and forest monitoring systems have evolved to levels in which accurate and precise global, regional to national loss estimates are derived from semi- automated or automated investigations of satellite imagery (Hansen et al. 2013; P. V. Potapov et al. 2014). Landsat 30-m spatial resolution satellite imagery have been used on large scales to show sub-hectare changes in land cover at excellent coverage and archived freely (Krylov et al. 2018).

Kenya has five major water towers namely Mount Kenya, The Aberdare Ranges, Mau forest complex, Mount Elgon and Cherangani hills (MOEF 2018) which formed the focus of this study. The study exploited space technology by classifying Landsat imagery into two classes of trees and non-trees in order to accurately detect changes in tree cover within the water tower boundaries. This will then allow for a well-coordinated, efficient and strategic planning among stakeholders to implement forest restoration programmes as well as execute conservation measures on threatened forests in a spatially explicit manner.

1.2 Problem Statement

Like any other East African country, Kenya's forests within the water towers have been subject to fragmentation as a result of duress from excision, exploitation and encroachment (Ongugo et al. 2014). Efforts to restore these forests are met with many challenges including disturbance of natural floral distribution where trees are planted in wrong places, a lack of coordinated effort from stakeholders, the community, the government and NGOs. All these are fuelled by non-existence of base maps showing area and locations of degraded areas to guide the conservation efforts.

It is therefore useful to map tree cover change within the water towers to establish a conservation baseline and a quick, efficient way to achieve this is by using geospatial technology. This research therefore aimed at mapping the extent to which tree cover has been lost across the five major water towers. This will provide the much needed statistics that will boost the understanding of future plans to clearly lay down effective, efficient and well informed conservation policies and strategies to execute restoration programmes. Moreover, it will guide procedures of prioritization and selection of critical areas to be restored with the aid of base maps showing degraded locations in the water towers over the past decade and a half from 2005-2019.

1.3 Objectives

The primary objective of this study was to monitor tree cover changes in the five water towers in Kenya using geospatial technologies.

Specific objectives

- To produce tree cover maps for each water tower at four epochs (2005, 2010, 2015 and 2019)
- To determine tree cover changes in each water tower between the epochs in terms of spatial distribution and quantities.
- To establish trends, if any, in tree cover losses in each water tower.
- To compare and contrast the overall tree cover losses among the five water towers.

1.4 Expected Results

- Maps of sites that have suffered tree cover loss in each water tower at each epoch.
- Estimates of quantities of tree cover lost for each water tower at each epoch.
- Trends of tree cover loss if any, in each water tower.
- A comparison of the overall losses of tree cover among the five water towers.

1.5 Justification for the Study

The findings of this study will provide the much needed tree cover loss statistics to government agencies as well as NGOs concerned with conservation, in order to establish a baseline for restoration and mitigation measures across the major water towers including prioritizing critical water towers that need urgent action. Moreover, the procedures could be translated to other water towers that have recently been gazetted with the similar aim of estimating tree cover loss statistics.

In addition, the results will provide room for further studies to investigate the natural and human-induced causes of tree cover loss or assess the effects of such losses to various aspects of the ecosystems dependent on these water towers.

1.6 Scope of work

The main focus of this study was to quantitatively analyse, map and compare tree cover loss across the five major water towers in Kenya for a period of 14 years from 2005-2019. The base year is a few years after the first UN World Summit on sustainable development, with a decade enough to detect substantial changes in tree cover. The research however, did not cover the underlying causes of tree cover loss, whether natural or human induced, but rather provided the statistics of what has been lost in terms of spatial locations, area and percentages.

2. LITERATURE REVIEW

2.1 Water towers

Originally, the term “water tower” was used to depict “a pillar holding a raised tank, whose height generates necessary pressure to distribute water in a piped system” (Duckett 2005). In a hydrological point of view, it is an emblematic term for a mountainous region that distributes disproportional-depending on angle the mountain is looked at- runoff in contrast to adjoining lowland areas (Viviroli et al. 2007).

A critical exposure the global society will encounter in future is fresh water access in adequate quantities and of satisfactory quality to meet the ever growing population and demand for food production (Wiegandt 2017). The consequence would be increased pressure on mountains that have always held a prerogative relation with water as the fountains of the world’s greatest water reservoirs.

It is believed that the majority of the rivers on earth emanate from mountain regions (Wiegandt 2017). In any particular region, mountain dispense can constitute as much as 50-90% of the global dispense of a catchment (Abaje et al. 2016). In a dynamic environment with growing population, the contribution of mountains in supplying water to lowland areas has to be pointed out more closely.

Strategies used to protect and manage water catchment areas have been heavily guided by various multilateral agreements (Harrison et al. 2016) that set targets to be followed by individual countries as those set by CBD strategic plan for biodiversity(CBD & Conference of Parties 2010). Geospatial technologies can be used to support such strategies through monitoring of critical catchments areas and forests as in the case of the Democratic Republic of Congo where forest cover loss was quantified using Landsat ETM+ to assess gross forest cover loss for the decade between 2000-2010 (Peter V. Potapov et al. 2012).

Fresh water is typically a common resource pool due to the fact that it is impractical, or exceedingly costly, to limit the rate of its use or the number of users. This inescapably results to possible “tragedy of commons” in cases where users reap benefits in the absence of paying for the cost of utilizing the resource (Hardin 2009). Studies conducted on small watersheds reveal that deforestation can surge annual runoff whereas afforestation impacts streamflow in a divergent way (Buendia et al. 2016; Carvalho-Santos et al. 2016; Zhang et al. 2016).

About 75% of Kenya’s renewable surface water emanate from the country’s water towers and catchments which are made up of forests (Kanui et al. 2016). They hence serve vital water regulation functions that are principal for irrigated agriculture, production of hydro-electric power and sustenance of human livelihoods.

The UN General Assembly proclaimed the period 2005-2015 as the global action decade termed “Water for life” (UN 2014), while at the same time the World Summit for Sustainable Development and Agenda 21 proclaimed the same period as the “International Decade for Education for Sustainable Development” (*World Summit Sustain. Dev.* 2005). The combination of the two is crucial for promise of management and preservation of water resources, including catchment areas.

To ensure adequate supply of fresh water, catchment areas have to be protected from destruction. On the other hand, action has to be taken to mitigate endangered catchment areas which can be only achieved if the extent of destruction is well understood, forming the basis for this research study. Kenya has five major water towers namely Mt. Kenya, Mt. Elgon, Cherangani hills, The Aberdare range and The Mau forest complex as outlined in Figure 3.2.

2.1.1 Mount Kenya

Mount Kenya is a solitary mountain of volcanic origin located on the equator 180 km north of Nairobi with a base diameter of approximately 120 km and a peak of 5199 m. It extends across six counties namely Meru, Embu, Laikipia, Kirinyaga, Nyeri and Tharaka Nithi. It plays a critical role in water catchment and is a source to two major rivers, Tana and Ewaso Ng’iro.

There are several vegetation bands with immense biological diversity from the mountain base to the summit that saw a total area of 715km^2 around the mountain center designated as a National park and listed as a UNESCO World Heritage Site in 1997.

The main economic activity of the people living around the water tower is small-scale farming directed at production of tea, coffee, maize, beans, potatoes and vegetables as well as dairy and mixed livestock farming. Other than water supply, the residents also enjoy a variety of ecosystems services both tangible, like wood and non-wood products, and intangible services like micro climate regulation.

2.1.2 Mount Elgon

Mount Elgon is an extinct shield volcano that borders Uganda and Kenya, north of Kisumu and West of Kitale with a base diameter of approximately 80 km and a highest peak of 4321 m. Unlike Mount Kenya, it extends across only two counties, Bungoma and Trans-Nzoia, but plays a crucial role in water catchment as well giving rise to two major rivers, Nzoia and Turkwel which are important watersheds for Lake Victoria and Lake Turkana basins respectively

The mountain is also rich in biodiversity supporting over 37 globally threatened faunal species. The mountain supports small-holder farming which is the major economic activity around this water tower with a mix of livestock keeping, and is the main source of livelihood for indigenous Sabaot and Ogiek communities.

2.1.3 Cherangani hills

Cherangani hills forest is a collection of 12 forest blocks with a total of 120,841 Ha spanning three counties, West Pokot (31%), Trans-Nzoia (2%) and Elgeyo Marakwet (67%). The water tower hosts critical headwaters for rivers Nzoia, Turkwel and Kerio which drain into Lake Victoria and Lake Turkana water basins.

The hills are an important biodiversity hotspot known to harbour several forest types and regionally threatened animal species such as the red chested owlet and the African crown eagle. The buffer zone around the water tower provides high agricultural potential support crop and livestock production

2.14 The Aberdare range

The Aberdare range is a 160 km long mountain range north of Kenya’s capital Nairobi. With an average elevation of 3500 m, it is located in west central Kenya, just south of the equator and situated in Nyandarua County. The water tower serves as a catchment to rivers Athi, Tana, Ewaso Nyiro and Malewa and has three distinctive vegetation zones including closed canopy forest belt, the bamboo zone and the alpine vegetation. In addition, it supplies most water consumed in the capital city, Nairobi, through Ndakaini and Sasumua dams.

Reliable rainfall and fertile soils around the forest reserve provide high potential for farming which is the main economic activity in adjacent communities as well as supporting livestock production especially dairy.

2.1.5 The Mau forest complex

The Mau forest complex is situated at 0°30’ South, 35°20’ East in the Rift Valley province spanning over five counties namely Bomet, Nakuru, Kericho, Narok and Uasin-Gishu with a combined forest coverage of over 400,000 ha. It is known to be the largest remaining closed canopy forest block in East Africa and serves as a catchment to many major rivers including Mara, Sondu, Yala, Nyando, Molo, Ewaso Ngiro, Nderit, Njoro, Makalia and many others.

The water tower comprises of 22 forest blocks and is known to support numerous biodiversity and ecosystems like the famous Mara-Serengeti ecosystem which is a major trans-boundary tourist attraction supporting millions of livelihoods. In addition to this, the favorable climate around the forest provides opportunity for small scale farming by people around it as well as livestock and dairy production.

2.2 Tree cover dynamics and impacts

Climate and land cover (along with soils, topography etc.) have been acknowledged as dominant controls of surface water balance, chiefly in the splitting of precipitation into evapotranspiration and runoff events (Williams et al. 2012). However, observations are still required to describe the precise nature of their controls across broad geographic domains (Kleidon 2008).

Techniques to evaluate the consequences of vegetation elimination on streamflow reciprocation including peak flows, low flows and specifically annual water yields have been achieved through paired catchment studies (Stednick 1996). Solutions to water availability and cooling effect are, as illustrated by Figure 2.1, functions inherent to forests (Ellison et al. 2017; Syktus & McAlpine 2016). Scientific evidence distinctively culminates substantial reduction in streamflow as a consequence of reforestation and afforestation, while forest logging intensifies streamflow (Andréassian 2004; Farley et al. 2005).

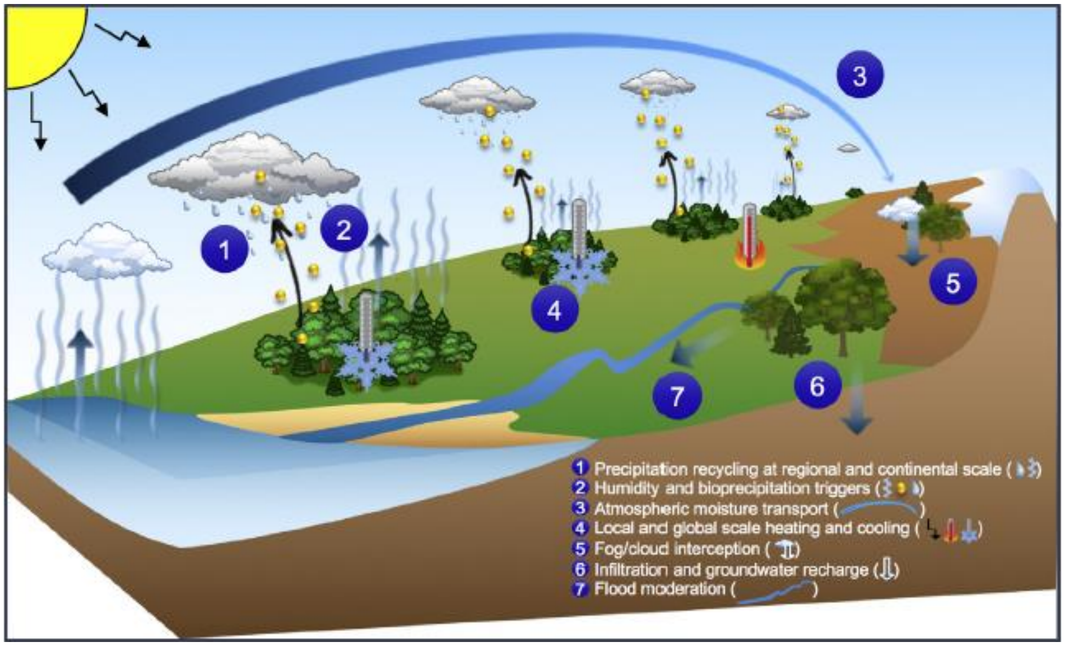

Figure 2.1 Impacts of forests on water and energy cycles (Ellison et al. 2017)

It has been noted by (FAO, 2015) that the global forest cover amounts to just a third of the earth's surface. In Kenya, it is said to be currently at 7.4% (MOEF, 2018) of the total land area which is below the 10% constitutional requirement despite the fact that they contribute to 3.6% of the country's GDP, except direct subsistence use and charcoal production (Kanui et al. 2016). Moreover, the forests directly and indirectly support service and productive sectors of national and local economies specifically trade, industry, tourism, water, wildlife, energy, livestock, fisheries and agriculture that are known to contribute 33-39% of the country's GDP (MOEWNR 2014). Kenya's closed canopy forest cover is presently estimated at 2% of the total land area, situated in montane forests that are the nation's water towers, in contrast to Africa's average of 9.3% and a world average of 21.4% (MOEF 2018).

There have been concerns about lifelong deterioration of natural Earth system roles as a result of land use modification and deforestation which have key implications to livelihoods sustainability, species survival, climate and ecosystems (Steffen et al. 2015). It is known that deforestation incapacitates the local hydrological cycle and the result being new heat patterns occurring as a result of changed land cover(Werth & Avissar 2005). Kenya's forest report by the Ministry of Environment outlines that the forests have been alarmingly diminished at a rate of almost 5000 ha per annum. This trend is expected to lead to an annual depletion of water availability by close to 62 million cubic meters, translating to an economic loss of over USD 19 million (MOEF 2018).

Limited studies have been conducted to assess the level of tree cover loss within Kenya's forests situated in the water towers. Therefore, this study was aimed at exploiting this lack of information to provide statistics on how much tree cover has been depleted over the past decade.

2.3 Land-use and Land-cover analysis

How we utilize our forest resources has serious implications to the ability of these resources to sustain mankind for generations to come. In order to ensure our ultimate survival in future, it is important to monitor how we use these forest resources and the best, most efficient way to achieve this is by applying remote sensing techniques.

Over the past quarter century, development of advanced information management technologies, new satellites and sensors as well as image interpretation techniques have rapidly evolved remote sensing capabilities (Bill 2018). Availability of a variety of high and moderate spatial resolution images and different spectral resolutions allow users to discern more attributes of land cover in LULC mapping.

IPCC requires countries to develop national MRV systems to provide estimates of forest carbon stock loss as a result of degradation. In doing so, it recommended the combination of Earth observation (EO) data and field-based inventories to estimate the forest area changes (Penman et al. 2003).

Remote sensing techniques allow enhanced interpretation of satellite imagery to construct long time-series datasets (Mitchell et al. 2017). These datasets play a vital role in tracking forest disturbance from long term assessment of forest dynamics in response to natural and anthropogenic disturbances through change detection analyses.

Use of pre- and post-disturbance classified satellite imagery for change detection is normally limited to detection of wide scale change. However, when the spectral signals are analysed over a longer period of time, change detection can be more powerful in addition to improved signal-to-noise ratio for detection of subtle forest cover changes (Kennedy et al. 2010).

The fundamental principle for post-classification comparison techniques, the most used change detection technique, is vegetation index image differencing. A pixel of any particular band is subtracted from the twin pixel of the same band, but differ in imaging dates (temporal resolution). The principle underlying this technique is reliant on the idea that vegetation indices are related to abundance of biomass hence an increase or decrease in vegetation can be detected by differentiating the images (initial state image and final state image) (Nunes & Caetano 2006).

Based on this concept, Landsat-based Detection of Trends in Disturbance and Recovery draws out spectral course of change using Landsat datasets. Slow and abrupt change events, (regrowth and harvesting respectively), can be detected by applying fitting strategies and temporal segmentation. As a result, reconstruction of continuous forest monitoring and disturbance history at national or local scales with more recent observations is enabled (Huang et al. 2009).

This study applied principles of a remote sensing technique whereby features and objects on the earth's surface are detected and discriminated by recording radiant energy reflected by these objects or features. It is built on the principle that different objects return different amounts of energy in different electromagnetic spectrum bands incident upon them. This principle made possible the differentiation of surfaces with tree cover from those without in order to monitor tree cover changes in Kenya's five major water towers through the study period.

3. MATERIALS AND METHODS

The methodological flow of the study is outlined in Figure 3.1

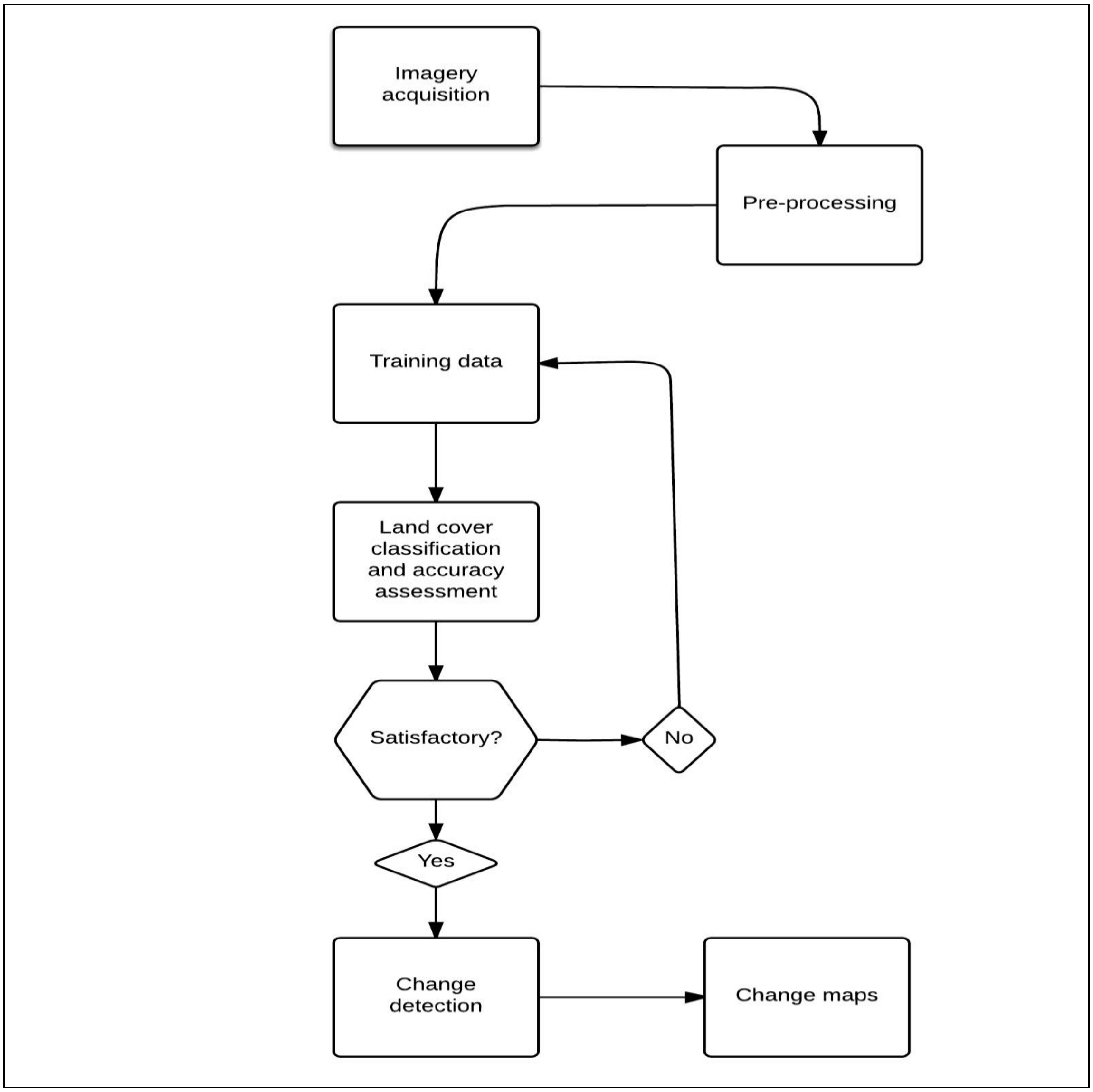

Figure 3.1 Methodology flowchart

3.1 Study areas

The study was conducted on Kenya's five major water towers within the boundaries provided by KWTA as shown in Figure 3.2. Cherangani hills water tower covers approximately 1,206 km^2, Mt. Kenya 1,992 km^2, Mt. Elgon 1,065 km^2, Aberdare range 2,820 km^2, and Mau complex 4,035 km^2 making a total of 11,118 km^2.

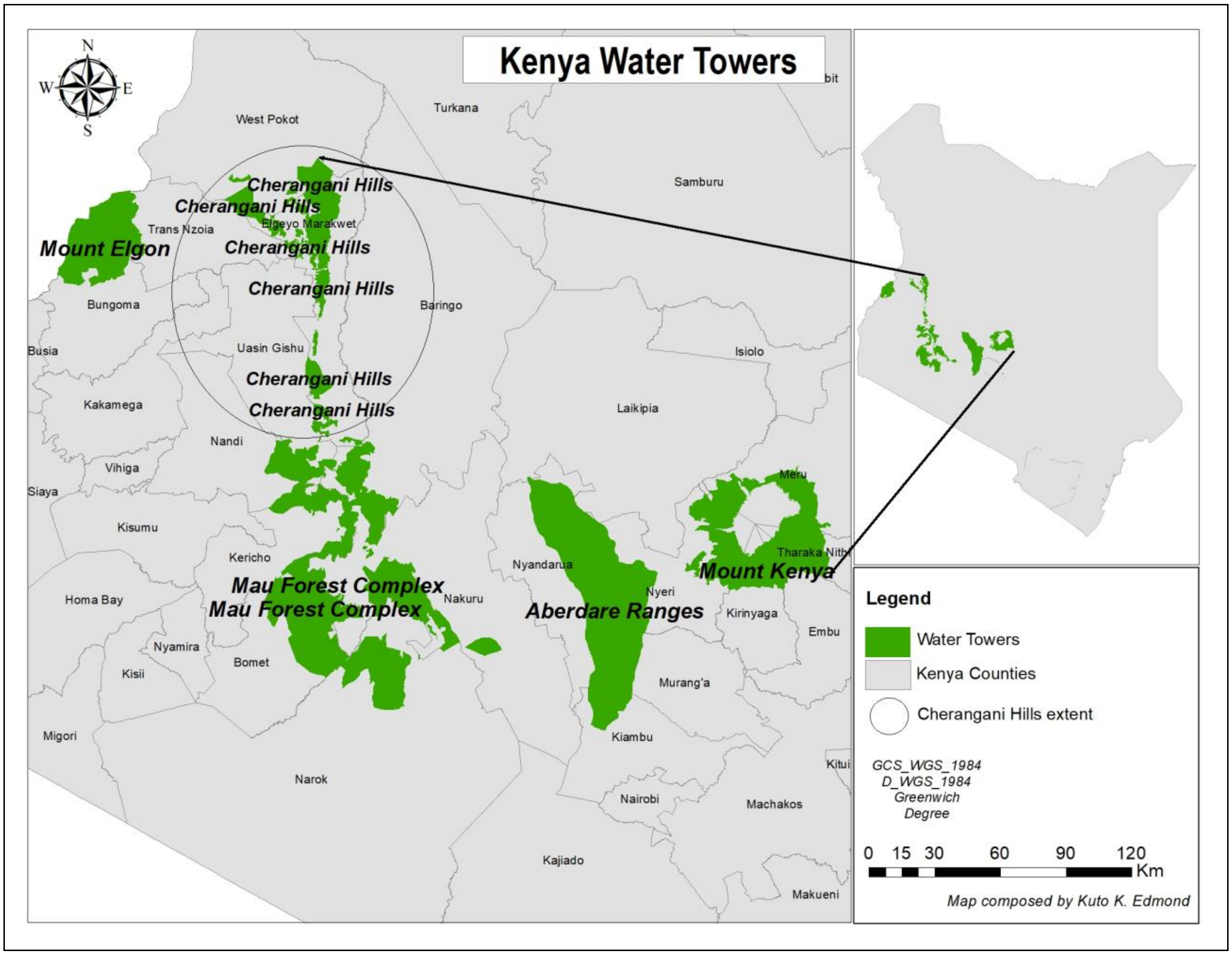

Figure 3.2 Map showing the water towers in Kenya

3.2 Data requirements

The study exploited most of secondary data sources from remote sensing and government archives whose specifications are outlined in Table 3.1.

Table 3.1 A summary of the data used in the study.

Data	Type	Source	Spatial Resolution	Acquisition date
Landsat Images	Raster	USGS, Google Earth Engine	30 m	2005-2019
Contemporary Images	Raster	KWTA	1.5 m	2019
Water tower boundaries	Vector	KWTA		2019

3.3 Land cover classification

Robust classification methods are necessary in remote sensing for land cover monitoring to provide a means for precisely mapping complex LULC categories. The study period was grouped into five year intervals and their images classified into tree and non-tree cover classes using the RandomForest (RF) algorithm outlined in Equations 3.1 and 3.2 (Rodriguez-Galiano et al. 2012).

RF combines several classifiers whereby each classifier contributes one vote in assigning the most recurrent class to the input vector $(\mathbf{X})$,

$$(\mathbf{X})\hat{C}_{rf}^{B} = \textit{majority vote } \{\hat{C}_b(\mathbf{X})\}_1^B, \tag{3.1}$$

Where $\hat{C}_{rf}^{B}$ is the most recurrent class and $\hat{C}_b(\mathbf{X})$ is the class probability of the b_{th} tree of the random forest. Trees are used as base classifiers in the classification,

$$\{h(x, \Theta_k), k=1,\ldots,\}, \tag{3.2}$$

Where h is the decision tree, x is the input vector and $\{\Theta_k\}$ the random vectors that are unconstrained and uniformly distributed.

To maximize measurement of dissimilarity between classes, tree design requires selection of suitable attributes. Unlike regular methods of regression like the partial least squares regression or principal component, which can perform fine in high dimensional spectral data learning tasks but cannot directly eliminate features that are irrelevant, the RF classifier and it's Gini feature importance (Breiman 2001), well known as Gini index, on the other hand allows direct feature elimination.

In order to achieve direct feature selection, the RF classifier uses a small subset of "fit variables" used as training for classification purposes only hence its high level performance in regard to high data dimensions. A higher ranking or spectral features can then be achieved which performs well as a popular indicator of feature relevance.

At every node τ, within the binary trees T of the RF, The Gini impurity $i(\tau)$ sought the optimal split which measures how well a potential split is separating samples of the two classes in this specific node.

$Pk = \frac{nk}{n}$ is a fraction of n_k samples from class $k = \{0,1\}$ out of the total n samples at node τ, the Gini impurity $i(\tau)$ is calculated using Equation 3.3.

$$i(\tau) = 1 - p_1^2 - p_0^2 \tag{3.3}$$

Its decrease Δi that results from splitting and sending the samples to two sub-nodes τ_l and τ_r (with respect to sample fractions $Pl = \frac{nl}{n}$ and $Pr = \frac{nr}{n}$) by a threshold t_θ on variable θ is defined in Equation 3.4

$$\Delta i(\tau) = i(\tau) - p_l i(\tau_l) - p_r i(\tau_r) \tag{3.4}$$

A maximal Δi is determined by a comprehensive search of the pair {θ, tθ} from all variables θ at the node, as well as over all possible thresholds tθ. The decrease in Gini impurity resulting from this optimal split Δi_θ (τ, *T*) is recorded individually for all variables θ, and accumulated for all nodes τ in all trees *T* in the forest, as outlined in Equation 3.5

$$I_G(\theta) = \sum_T \sum_\tau \Delta \mathrm{i}_\theta(\tau, T) \tag{3.5}$$

I_G, the Gini importance, eventually indicates the number of times a particular feature θ was selected for a split, and how big its general preferential value was for the classification issue being studied.

Classification was carried out in a single merged image of all the water towers for each specific year of study. The training samples were collected randomly but picked from all the water tower boundaries to ensure diversity of class samples representing both tree cover and non-tree cover classes.

3.4 Land cover validation

Assessment of accuracy is a vital part in remote sensing for thematic mapping. It is far from a trivial process as numerous factors impart classification accuracy (Strahler et al. 2006). In relation to this debate, it is key to note that the size of samples for accuracy assessment in remote sensing vary substantially. Such variations contemplate partly issues like differences in needs and aims of the project as well as pragmatic constraints and limitations such as image quality and resolution (Foody 2009).

Bagging was used to select each subset using up to 2/3 of measurement dataset to make each individual b_{th} tree grow and the remaining 1/3 incorporated to another subset known as out-of-bag (OOB). For each b_{th} tree, a distinct oob subset was created from unselected components via the bootstrapping procedure and were not evaluated for training of the b_{th} tree. The purpose for this was to use the oob subset to evaluate performance which was a proportion of the overall number of oob elements and the misclassifications thus ensuring an impartial estimation of the error of generalization (Breiman 2001).

Of all the training sites, a third of the total samples were automatically and intentionally not picked for training to allow for out of bag (OOB) error estimates for accuracy assessment outlined in Tables 4.1 and 4.2. The sample sizes vary due to image quality variations whereby images for the years 2005 and 2010 were of low quality as compared to those of 2015 and 2019.

3.5 Change detection

The change detection process' main function is to recognize LULC on digital images that change features of interest between two or more dates. This was achieved through application of multi-temporal data sets to differentiate areas of land cover change between dates of imaging. Tree cover change detection was based on overlapping areas in earliest and latest classified maps and the post-classification comparison of independent classified images were used to assess tree cover area changes in all the five water towers.

3.6 Statistical analysis

Change detection statistics were used to compile detailed tabulation of changes between two classification images. Primarily, the focus was the analysis of previous state changes in classification whereby, for every prior state class, the pixels that changed for those classes were identified in the final state image. The results then enabled trend analysis of tree cover between the four epochs for each of the water towers and further compared tree cover change among the five water towers. Trends, (**T**), between any two epochs were identified using percentage difference which is a function of final state and initial state classes as outlined in Equation 3.6,

$$\boldsymbol{T} = \frac{f - i}{i} \tag{3.6}$$

where $\boldsymbol{f}$ is the number of pixels in the final state class and i the number of pixels in the initial state class.

4. RESULTS AND DISCUSSIONS

This chapter describes and discusses the results obtained.

4.1 Data processing results

Multi-temporal sets of remotely sensed data have been used to study and classify land cover on areas of interest (Lucas et al. 2007). Landsat 7 images acquired from Google Earth Engine were classified using RF algorithm via RStudio programming software (see Appendix I and II). The results were tree cover maps within the water towers as shown in the maps in Figures 4.1, 4.2, 4.3, 4.4 and 4.5.

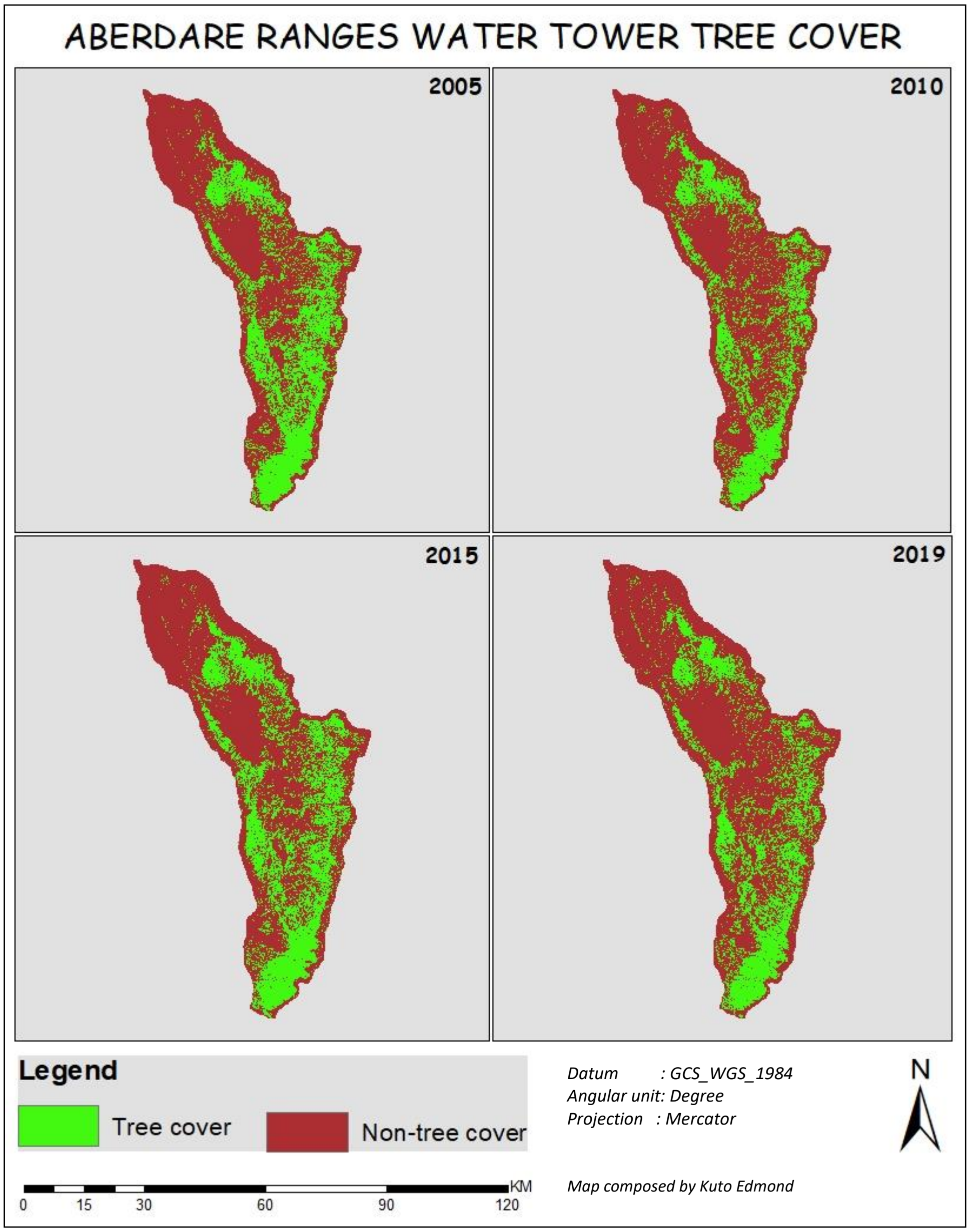

Figure 4.1 Map showing tree cover within the Aberdare range water tower

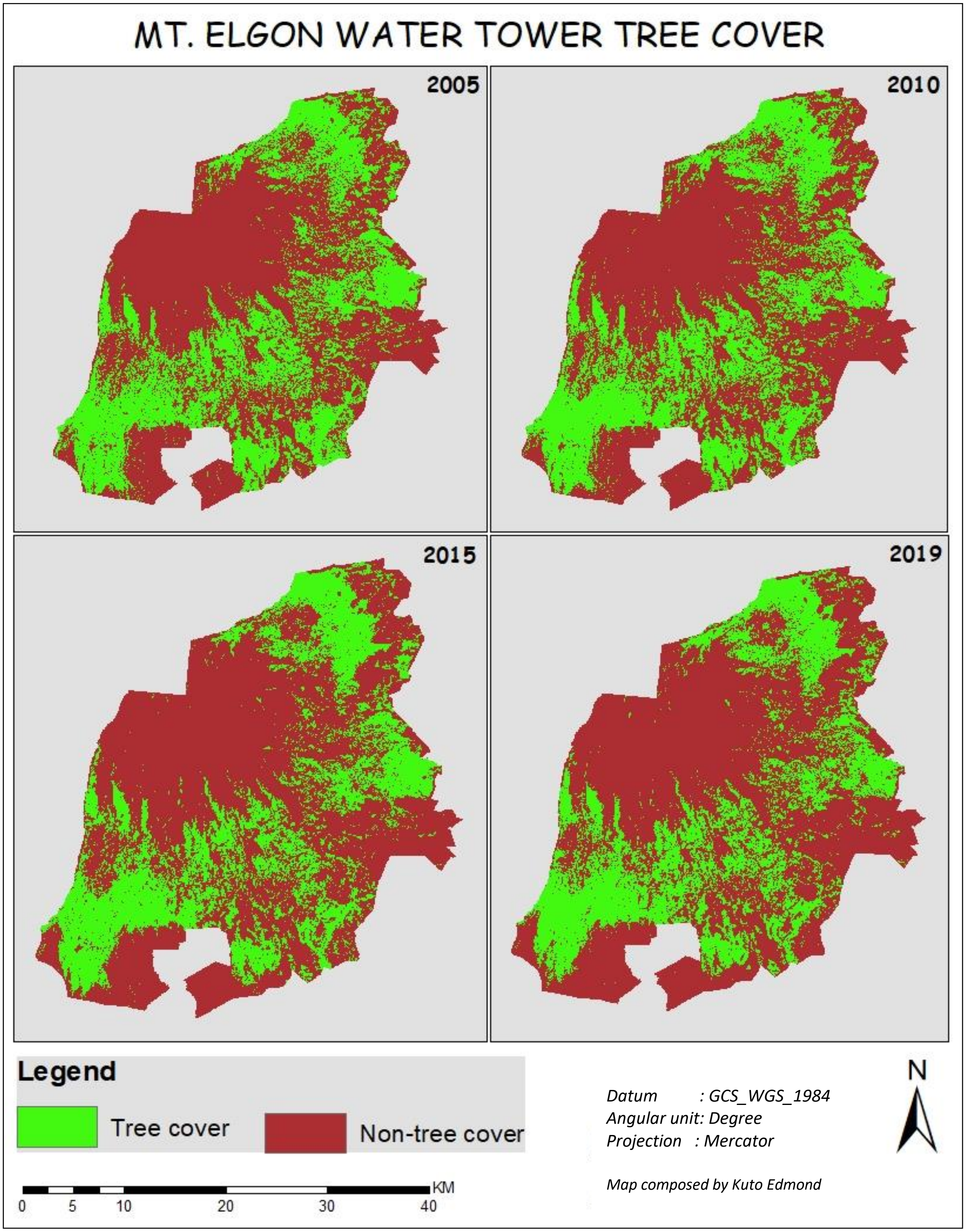

Figure 4.2 Map showing tree cover within Mt. Elgon water tower

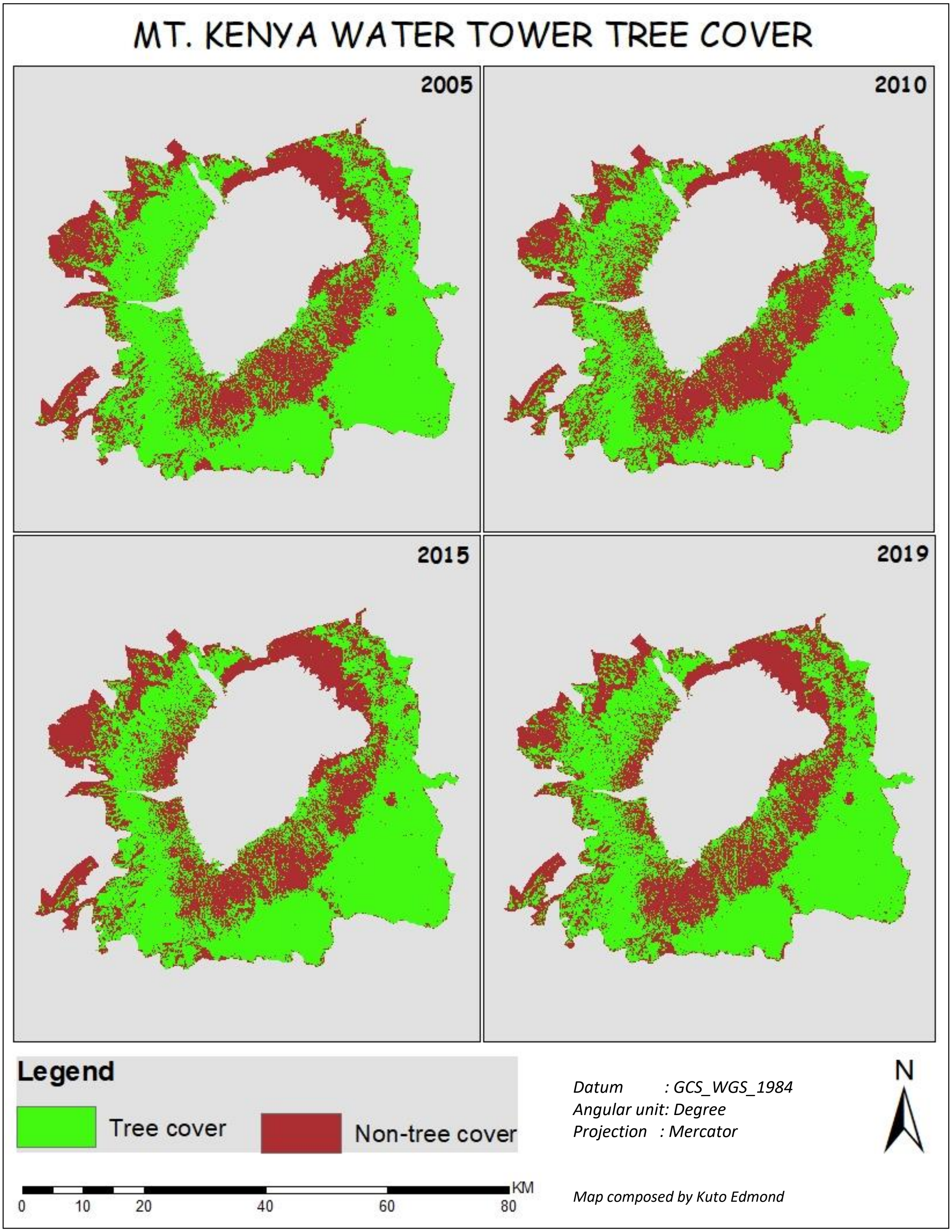

Figure 4.3 Map showing tree cover within Mt. Kenya water tower

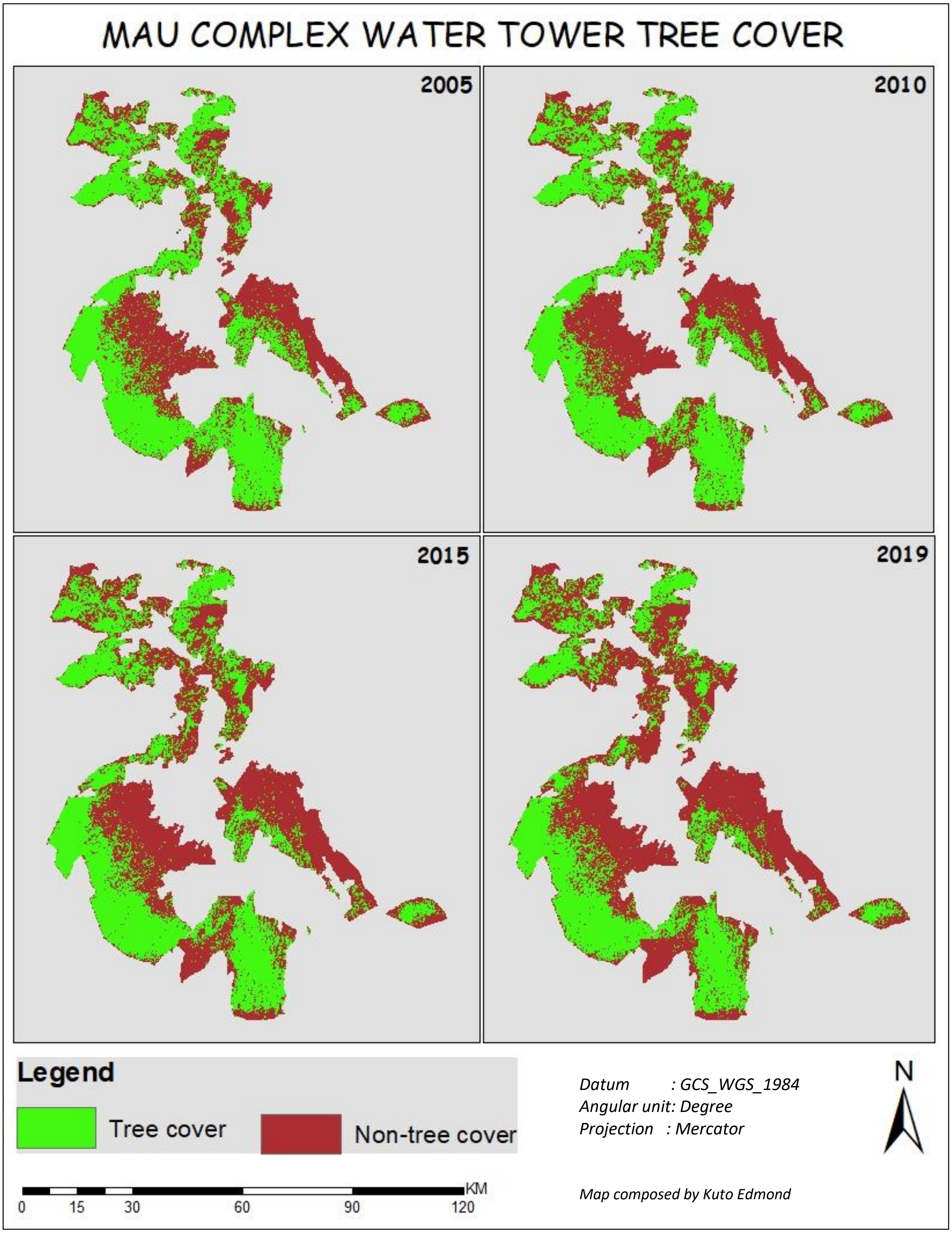

Figure 4.4 Map showing tree cover within the Mau forest complex water tower

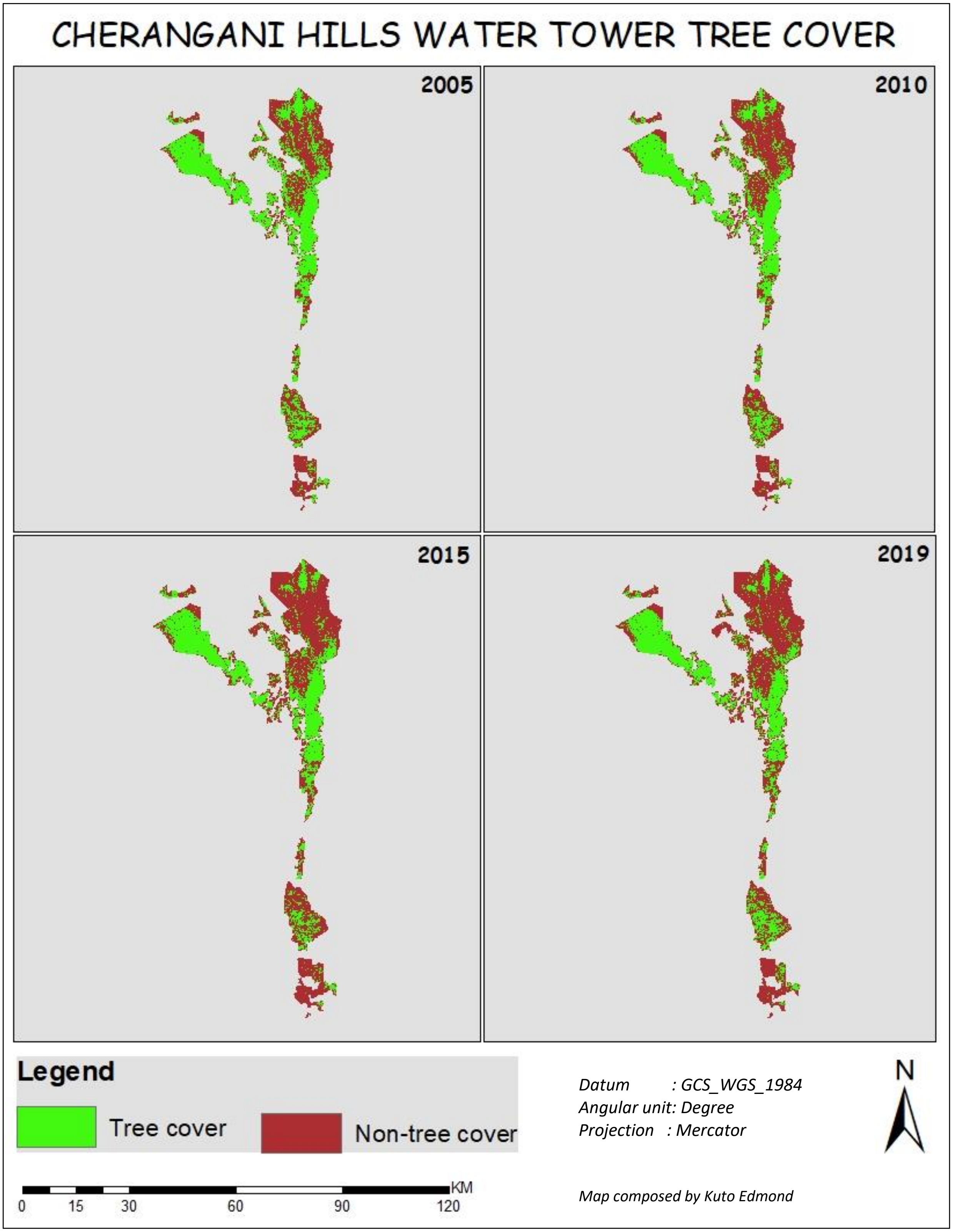

Figure 4.5 Map showing tree cover within the Cherangani hills water tower

4.2 Accuracy assessment

The results for the validation process are outlined in Tables 4.1 and 4.2. The classification performed very well with marginal OOB errors.

Table 4.1 Confusion matrix for years 2005 and 2010 classifications

	2005				2010			
	Class	1	2	Class error	**Class**	1	2	Class error
	1	1007	21	0.02042802	1	1005	8	0.00789734
	2	39	1000	0.03753609	2	12	1037	0.01143947
Sample size	130				128			

Table 4.2 Confusion matrix for years 2015 and 2019 classifications

	2015				2019			
	Class	1	2	Class error	**Class**	1	2	Class error
	1	1011	1	0.00098814	1	1011	2	0.00197433
	2	1	1021	0.00097847	2	5	1026	0.00484966
Sample size	75				78			

4.3 Change detection analyses

Auspiciously processed and elaborated remote sensing data can really be of importance in change detection assignment to track differences of land cover at contrasting times (Lu et al. 2004). Therefore, from the above dataset of multi-temporal classified images, digital change detection procedure permitted description and determination of changes in land cover between the four foundational intervals: 2005-2010, 2010-2015, 2015-2019 and overall 2005-2019.

Post-classification comparison, a GIS technique (Serra et al. 2003), was used to effectively integrate land cover maps and further quantitatively disclose change dynamics in each class category. Comparing the land cover data allowed generation of tables holding spatial information of every class about the nature of change, their location and amount (area) from the year 2005-2019.

4.3.1 Mount Kenya

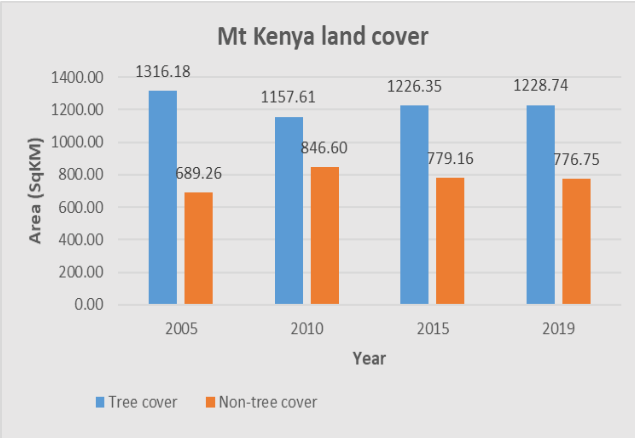

Figure 4.6 Mt. Kenya land cover area (km^2)

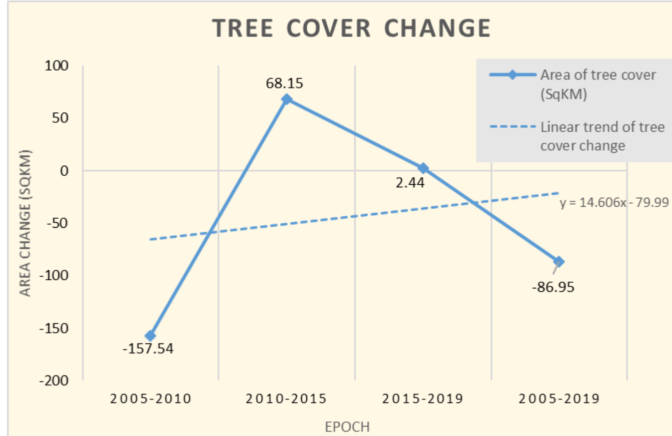

Figure 4.7 Mt. Kenya tree cover change (km^2)

The study discovered slight decrease in tree cover from 2005-2019 with an increase in tree cover between 2005-2015 before a further decline between 2015-2019 highlighted in Figures 4.6 and 4.7. The decrease in tree cover was overall witnessed at higher altitudes where human activities could not be the factor driving change leaving natural disturbance either from varying climatic conditions or other natural factors as shown in Figure 4.8. (Downing et al. 2017) established that more than 10% of the mountain burnt with the alpine section experiencing more than 33% over the last 16 or more years especially in the mooreland/grassland area.

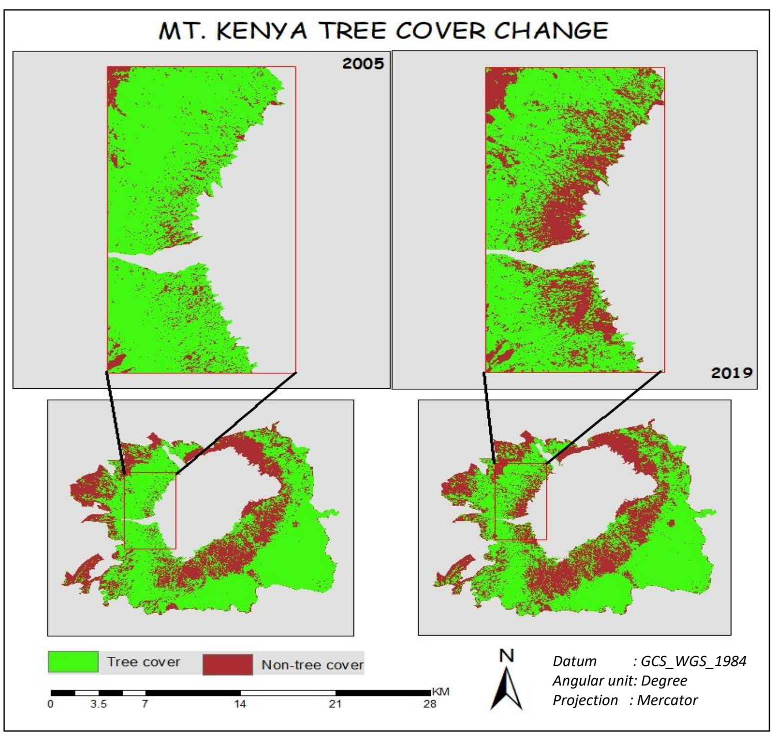

Figure 4.8 Mt. Kenya tree cover loss location

4.3.2 Mount Elgon

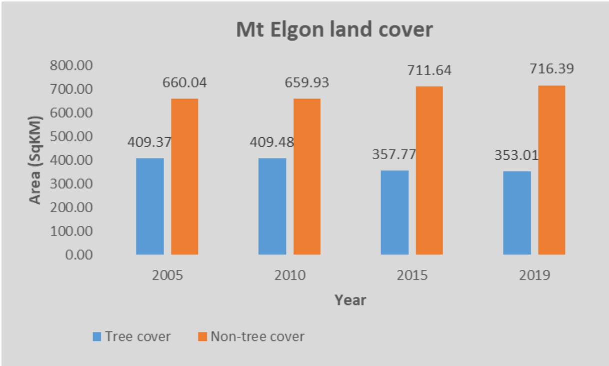

Figure 4.9 Mt. Elgon land cover area (km^2)

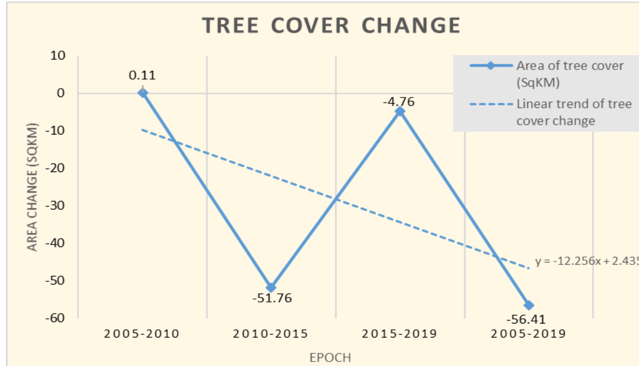

Figure 4.10 Mt. Elgon tree cover change (km^2)

Figures 4.9 and 4.10 show tree cover change in Mt. Elgon water tower. It has fairly been constant from 2005-2010 after which it experience a slight decline from 2010-2019 especially around the periphery, see Figure 4.11, where humans can easily access the forest hence suffered the most damage. A 2005 forest boundary resurvey found some people residing in the forest reserve (Soini 2007). Despite the communities' awareness of laws and regulations on forest use, (Kiragu 2002) discovered that few people extract forest products without necessary permits required by law. Such behavior could have led to the decline in tree cover along the forest boundary.

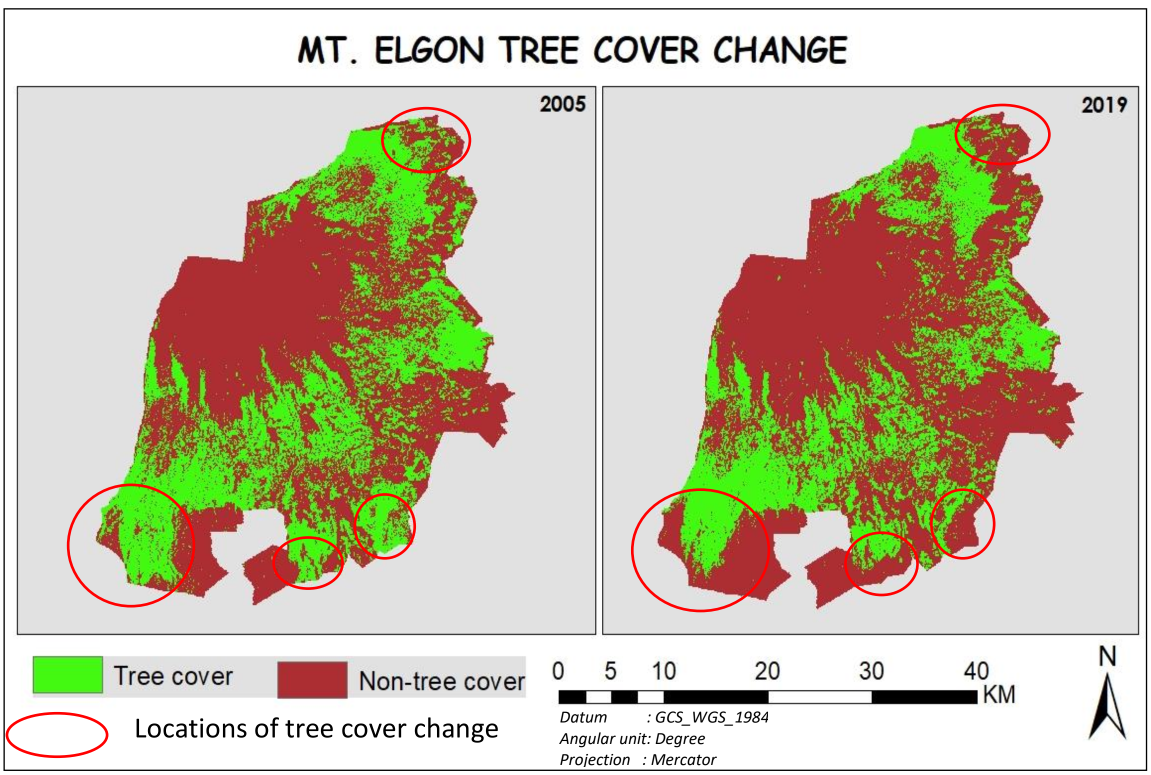

Figure 4.11 Mt. Elgon tree cover loss locations

4.3.2 Cherangani hills

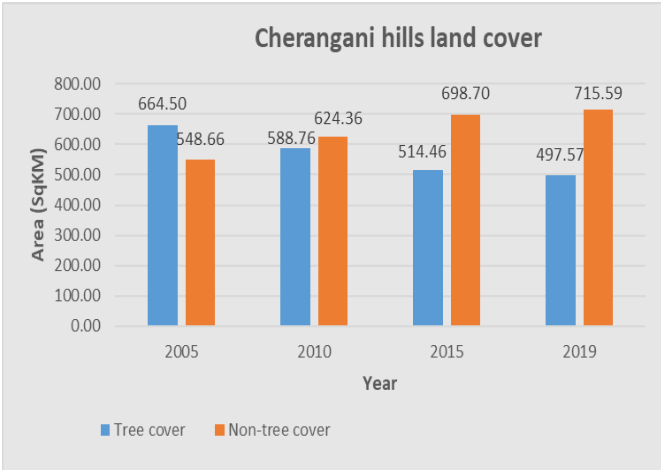

Figure 4.12 Cherangani hills land cover area (km²)

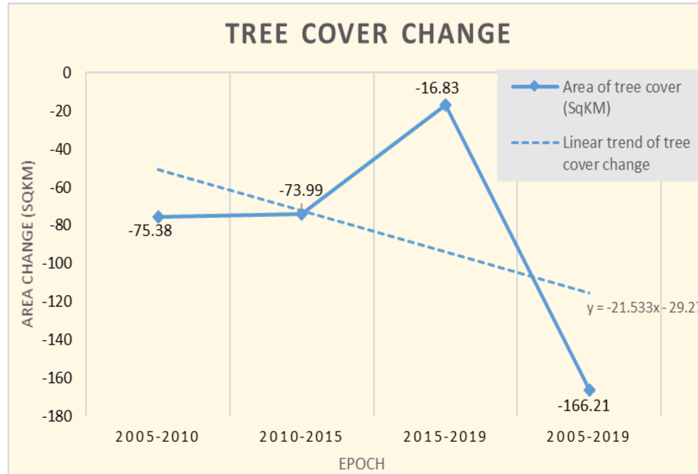

Figure 4.13 Cherangani hills tree cover change (km²)

Cherangani hills water tower experienced indiscriminate tree cover loss with a sharp decline from 2005-2019 evident in Figure 4.13. For every five years studied, it was found that there has been no point where tree cover increased visible in Figure 4.12. From the land cover maps, almost every location within the water tower boundary experienced loss evident in Figure 4.14.

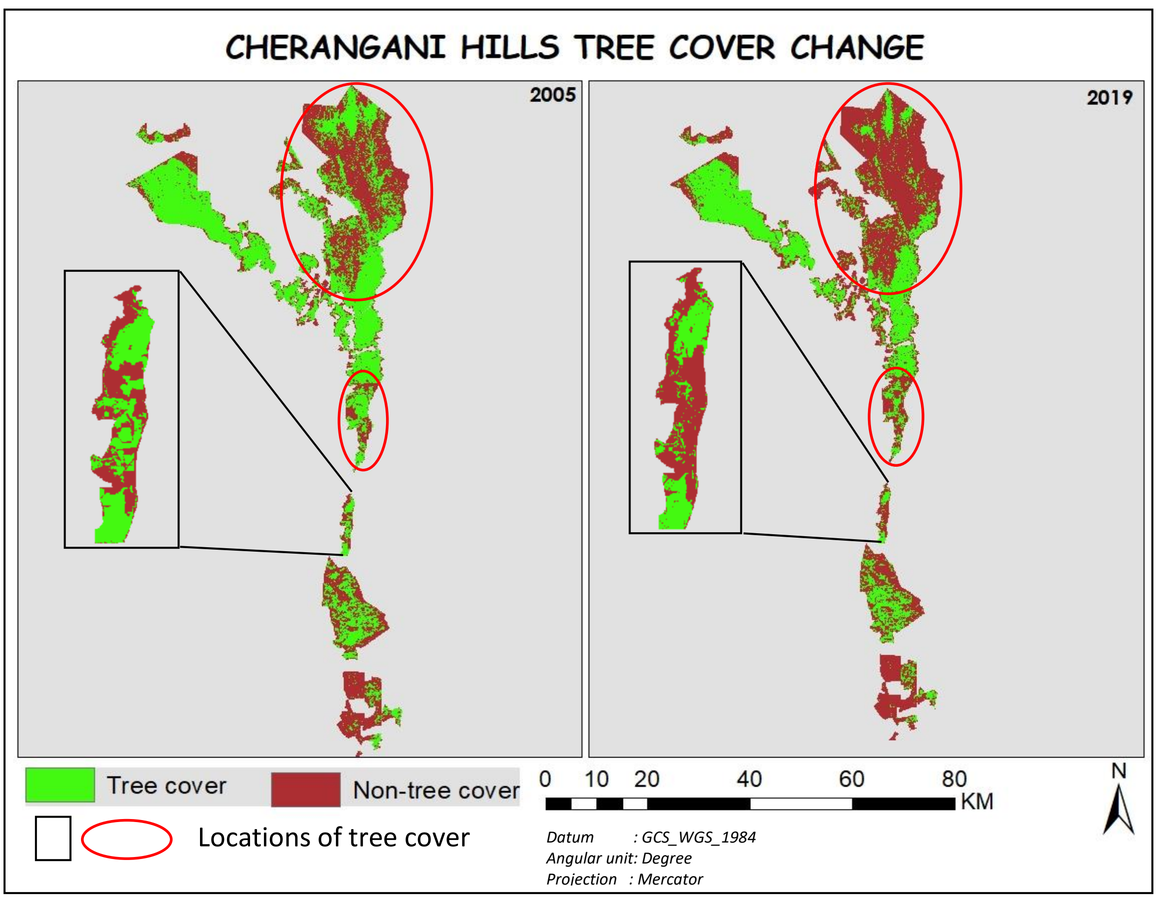

Figure 4.14 Cherangani hills tree cover loss locations

4.3.4 The Aberdare range

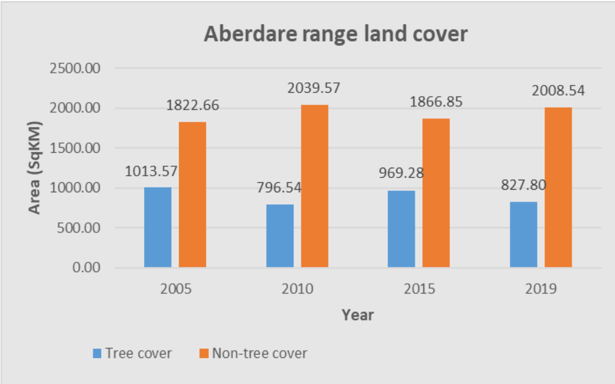

Figure 4.15 Aberdare range land cover area (km^2)

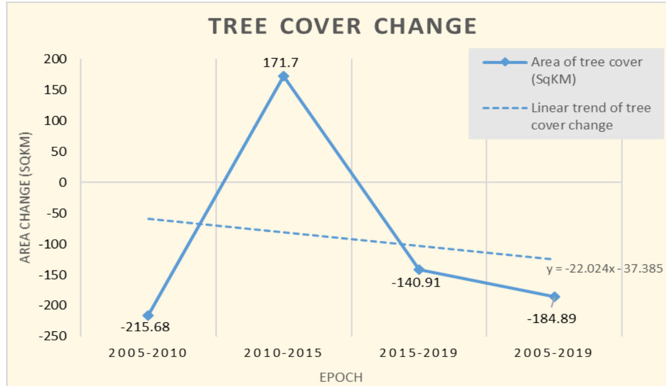

Figure 4.16 Aberdare range tree cover change (km^2)

The study identified tremendous decline in tree cover between 2005 and 2010 before and increase between 2010 and 2015. There was further drop from 2015-2019. The forest has had many plantations that might had seen such decline and increase in tree cover, as seen in Figures 4.15 and 4.16, as a result of harvesting and replanting respectively. In addition, excision, encroachment, illegal logging and charcoal making has further fuelled tree cover loss as outlined by (KFS 2010). The water tower's proximity to Nairobi city where demand for wood products is high is another factor that has seen increase in illegal logging within the forest boundary to meet such demands (Kegode 2009). The changes have occurred on small, scattered areas that when combined form large areas which is clear in Figure 4.17.

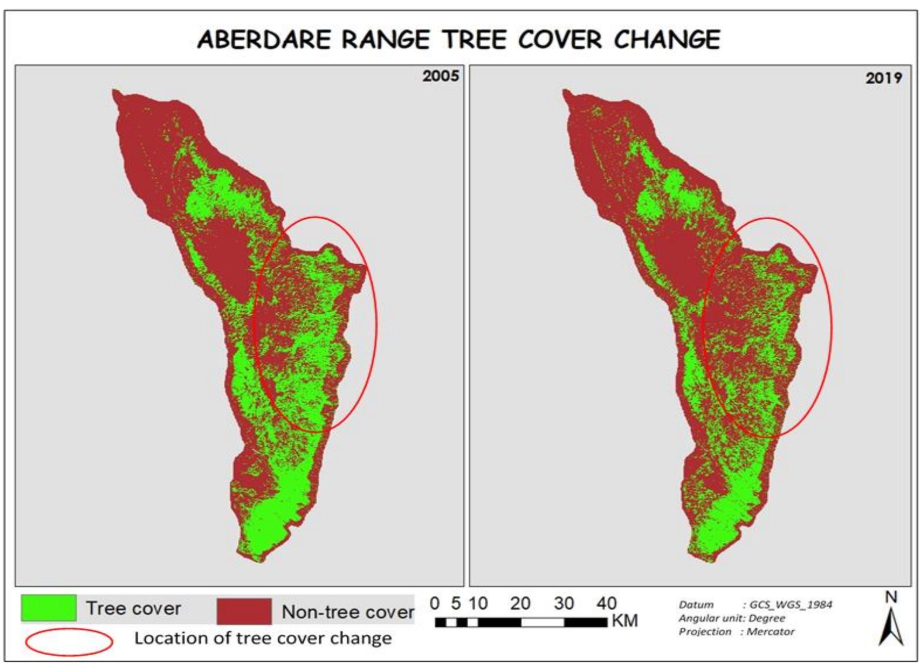

Figure 4.17 Aberdare range tree cover loss location

4.3.5 The Mau forest complex

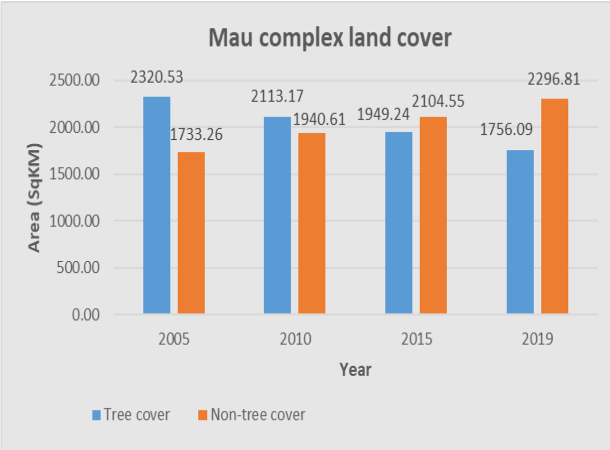

Figure 4.18 Mau forest complex land cover area (km^2)

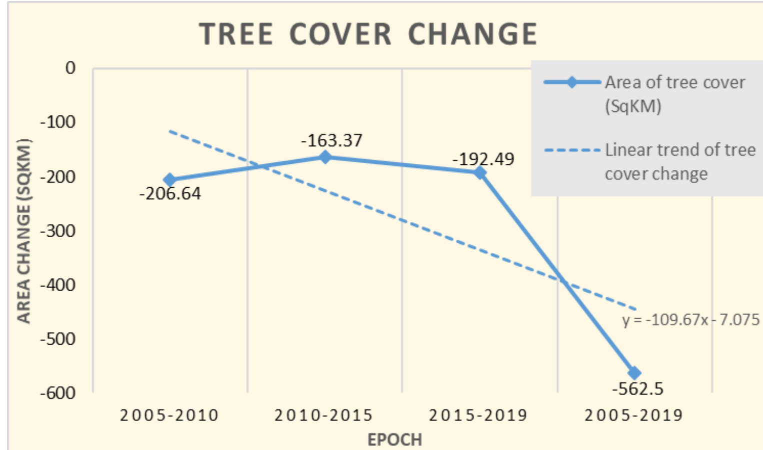

Figure 4.19 Mau forest complex tree cover change (km^2)

Tree cover within Mau forest complex experienced tremendous loss approximately over 560km^2 from 2005-2019 as shown in Figures 4.18 and 4.19. The study discovered the northern part of the water tower to have suffered the most visible in Figure 4.20. Such drastic declines in tree cover, as outlined by (Omondi & Musula 2011), is as a result of an upsurge of human population and their underlying activities. The result was increased conversion of land for agricultural activities and settlement over the years.

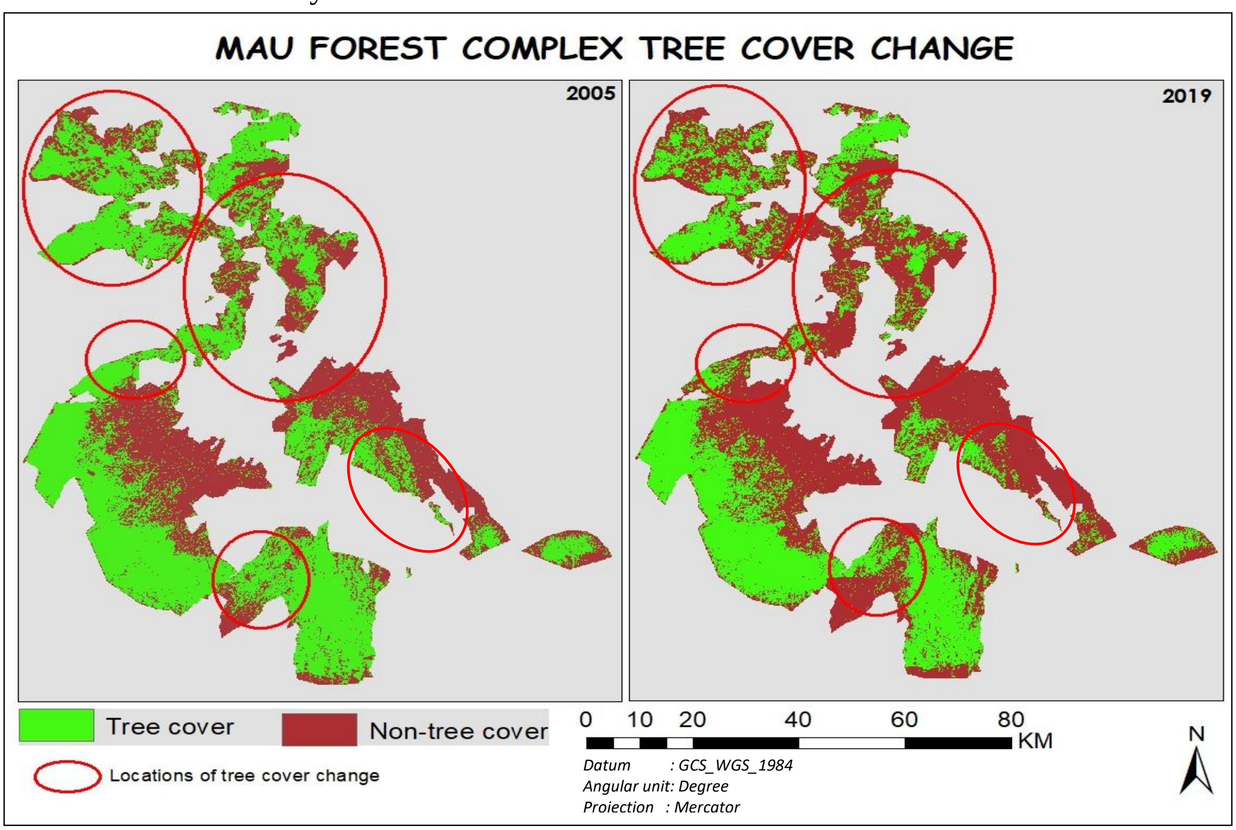

Figure 4.20 Mau forest complex tree cover loss locations

4.4 Trend analysis and tree cover loss comparison

Despite the positive and negative fluctuations in tree cover between the year intervals, the overall trend has been a decrease in tree cover among the five water towers evident in Figure 4.21.

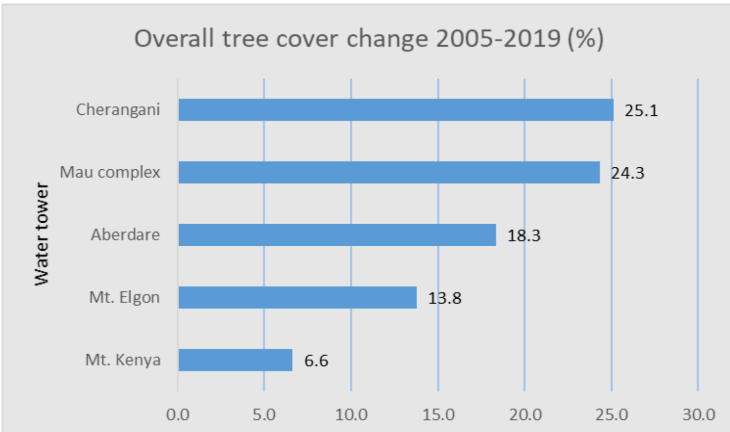

Figure 4.21 Overall decline in tree cover change

The study established the biggest losers of tree cover being Cherangani, Mau complex and Aberdare range water towers which experienced 25.1%, 24.3% and 18.3% respectively. Mt. Kenya saw the least change standing at 6.6% followed by Mt. Elgon at 13.8%.

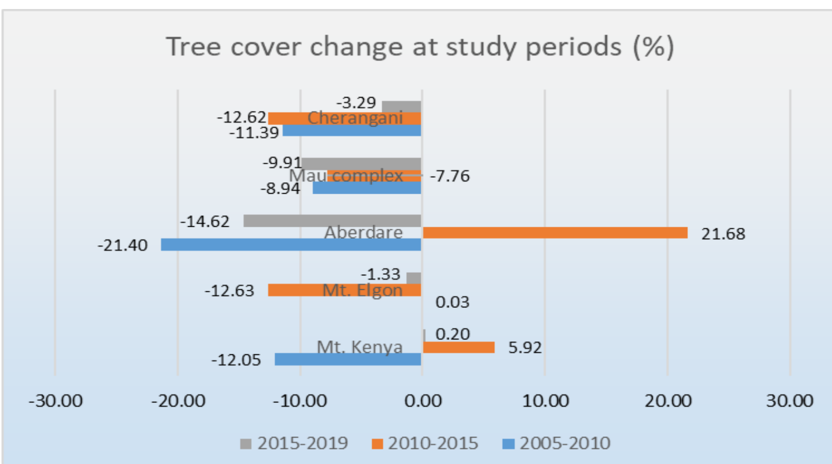

Figure 4.22 Tree cover change at study periods

Evident in Figure 4.22, the water towers have had substantial changes in tree cover. The period between 2010 and 2015 had some positive change witnessed at Aberdare range and Mt. Kenya with 21.7% and 6% tree cover increase respectively. There was an insignificant 0.2% increase of tree cover between 2015 and 2019 within Mt. Kenya and 0.03% increase in Mt. Elgon between 2005 and 2010. Cherangani hills and the Mau forest complex encountered a decline in tree cover across all the study periods. The period between 2005 and 2010 was also found out to be the leading in tree cover loss especially in Aberdare range water tower.

5. CONCLUSIONS AND RECOMMENDATIONS

5.1 Conclusions

The study established a decline of tree cover across all the water towers amounting to an average of 19% decline, which is approximately1061 km^2, from 2005-2019. These losses were witnessed mostly around the water tower peripheries where access by humans is easy. Of the five water towers, Cherangani hills and the Mau complex were found out to be the most degraded experiencing a tree cover decline of 25% and 24% respectively. This can be attributed to encroachment for agricultural expansion and illegal harvesting of trees.

Aberdare range was the third most degraded with 18% loss, a trend fuelled by increasing demand of wood products within Nairobi city, which results to illegal logging in the forest. On the other hand, Mt. Elgon and Mt. Kenya were the least disturbed standing at approximately 14% and 7% respectively. Fire has been a major concern and cause of tree cover loss within Mt. Kenya water tower, especially the moorland area, whereas loss at Mt. Elgon can be attributed to human encroachment seeking to expand agricultural land.

Such trends of tree cover decline within the water towers will endanger our already water stressed society. Trees play a major role in evapotranspiration and interception of rainfall that facilitates percolation by reducing splashing and runoff and further enhancing ground water recharge. This therefore means that low tree cover in the water towers would put at risk the country’s access to fresh water which is a fundamental right and a basis for life.

5.2 Recommendations

The government and NGOs need to apply geospatial techniques in identification and location of potential rehabilitation areas in their efforts to save these forests. This will allow these authorities to maintain and preserve the natural distribution of flora that directly affect survival of fauna and prevent habitat loss and extinction of critically endangered species.

While Landsat imagery with moderate 30-m spatial resolution provide a basis to detect and track tree cover changes over a longer time period, it is appropriate to integrate with current era better spatial resolution imagery at no cost. Studies aimed at execution of restoration programs should combine both moderate and a bit higher resolution open-source imagery, for example 10-m resolution Sentinel images available from the year 2015 onwards. This will enable proper identification of more detailed locations and area of degraded areas which is critical for informed planning.

The sample size used for training was low, taking into consideration the study area. A similar study for restoration programmes could opt for a larger sample size to ensure a more heterogeneous representation of classes. Furthermore, additional land cover classes could be introduced to distinguish actual tree cover to more similar classes such as higher shrubs and grasses (bamboo) which can be classified as trees.

REFERENCES

Abaje, I., Sawa, B., Iguisi, E., Ibrahim, A., Bekele-, A., Coleridge, P., KU(Kenyatta University), et al. (2016). *Mountains Vulnerable of the World : Water Towers for the 21st Century*. *Conservation Biology*. DOI: 10.1017/CBO9781107415324.004

Andréassian, V. (2004). 'Waters and forests: From historical controversy to scientific debate'. *Journal of Hydrology*. DOI: 10.1016/j.jhydrol.2003.12.015

Bainbridge, D. A. (2017). 'Global Guidelines for the Restoration of Degraded Forests and Landscapes in Drylands: Building Resilience and Benefitting Livelihoods', *Restoration Ecology*. DOI: 10.1111/rec.12483

Bill, R. (2018). 'Remote sensing and GIS'. *gis.Science - Die Zeitschrift fur Geoinformatik*. DOI: 10.1201/9780429326349-15

Breiman, L. (2001). 'Random forests', *Machine Learning*. DOI: 10.1023/A:1010933404324

Buendia, C., Batalla, R. J., Sabater, S., Palau, A., & Marcé, R. (2016). 'Runoff Trends Driven by Climate and Afforestation in a Pyrenean Basin', *Land Degradation and Development*. DOI: 10.1002/ldr.2384

Carvalho-Santos, C., Nunes, J. P., Monteiro, A. T., Hein, L., & Honrado, J. P. (2016). 'Assessing the effects of land cover and future climate conditions on the provision of hydrological services in a medium-sized watershed of Portugal', *Hydrological Processes*. DOI: 10.1002/hyp.10621

CBD, & Conference of Parties. (2010). 'Strategic Plan for Biodiversity 2011-2020, including Aichi Biodiversity Targets'. *The Convention on Biological Diversity*. DOI: 10.1007/978-94-007-4032-7

Downing, T. A., Imo, M., & Kimanzi, J. (2017). 'Fire occurrence on Mount Kenya and patterns of burning', *GeoResJ*. DOI: 10.1016/j.grj.2016.12.003

Duckett, B. (2005). ' Concise Oxford English Dictionary (11th edition)200532Edited by Catherine Soanes and Angus Stevenson. Concise Oxford English Dictionary (11th edition) . Oxford: Oxford University Press 2004. xx+1,708 pp., ISBN: 0 19 860864 0 £20.00 $29.95 ', *Reference Reviews*. DOI: 10.1108/09504120510573710

Ellison, D., Morris, C. E., Locatelli, B., Sheil, D., Cohen, J., Murdiyarso, D., Gutierrez, V., et al. (2017). 'Trees, forests and water: Cool insights for a hot world', *Global Environmental Change*. DOI: 10.1016/j.gloenvcha.2017.01.002

FAO. (2015). *Global Forest Resources Assessment 2015: How are the world's forest changing? FAO Forestry*. DOI: 10.1002/2014GB005021

Farley, K. A., Jobbágy, E. G., & Jackson, R. B. (2005). 'Effects of afforestation on water yield: A global synthesis with implications for policy', *Global Change Biology*. DOI: 10.1111/j.1365-2486.2005.01011.x

Foody, G. M. (2009). 'Sample size determination for image classification accuracy assessment and comparison', *International Journal of Remote Sensing*. DOI: 10.1080/01431160903130937

Geiling, N. (n.d.). 'Reforestation Doesn't Fight Climate Change Unless It's Done Right – ThinkProgress'. Retrieved February 8, 2020, from <https://thinkprogress.org/planting-trees-climate-change-solution-3e5b6979561f/>

Hansen, M. C., Potapov, P. V., Moore, R., Hancher, M., Turubanova, S. A., Tyukavina, A., Thau, D., et al. (2013). 'High-resolution global maps of 21st-century forest cover change', *Science*. DOI: 10.1126/science.1244693

Hardin, G. (2009). 'The tragedy of the commons', *Journal of Natural Resources Policy Research*. DOI: 10.1080/19390450903037302

Harrison, I. J., Green, P. A., Farrell, T. A., Juffe-Bignoli, D., Sáenz, L., & Vörösmarty, C. J. (2016). 'Protected areas and freshwater provisioning: a global assessment of freshwater provision, threats and management strategies to support human water security', *Aquatic Conservation: Marine and Freshwater Ecosystems*. DOI: 10.1002/aqc.2652

Horowitz, C. A. (2016). 'Paris Agreement', *International Legal Materials*. DOI: 10.1017/s0020782900004253

Huang, C., Goward, S. N., Schleeweis, K., Thomas, N., Masek, J. G., & Zhu, Z. (2009). 'Dynamics of national forests assessed using the Landsat record: Case studies in eastern United States', *Remote Sensing of Environment*. DOI: 10.1016/j.rse.2008.06.016

Kanui, T., Kibwage, J., & Murangiri, M. (2016). 'Water Tower Ecosystems Services and Diversification of Livelihood Activities to Neighbouring Communities; A Case Study of Chyulu Hills Water Tower in Kenya', *Journal of Geography, Environment and Earth Science International*. DOI: 10.9734/jgeesi/2016/26620

Kegode, H. (2009). 'Rehabilitation of the Aberdare Forest Ecosystem Midterm Review Report Green Belt Movement Rehabilitation of the Aberdare Forest Ecosystem', 203.

Kennedy, R. E., Yang, Z., & Cohen, W. B. (2010). ‘Detecting trends in forest disturbance and recovery using yearly Landsat time series: 1. LandTrendr - Temporal segmentation algorithms’, *Remote Sensing of Environment*. DOI: 10.1016/j.rse.2010.07.008

Kenya Forest Service. (2010). ‘Aberdare forest reserve managment plan’, 94.

Kiragu, S. W. (2002). *Community Participation in Forest Resources*. Moi Univesity.

Kleidon, A., & Germany, J. (2008). ‘Max-Planck Institute for Biogeochemistry Climatic constraints on maximum levels of human metabolic activity and their relation to human evolution and global change’, *Climatic Change*.

Krylov, A., Steininger, M. K., Hansen, M. C., Potapov, P. V., Stehman, S. V., Gost, A., Noel, J., et al. (2018). ‘Contrasting tree-cover loss and subsequent land cover in two neotropical forest regions: sample-based assessment of the Mexican Yucatán and Argentine Chaco’, *Journal of Land Use Science*. DOI: 10.1080/1747423X.2019.1569169

KWTA. (2019). ‘Kenya Water Towers Agency’. Retrieved from <https://watertowers.go.ke/>

Lu, D., Mausel, P., Brondízio, E., & Moran, E. (2004). ‘Change detection techniques’, *International Journal of Remote Sensing*. DOI: 10.1080/0143116031000139863

Lucas, R., Rowlands, A., Brown, A., Keyworth, S., & Bunting, P. (2007). ‘Rule-based classification of multi-temporal satellite imagery for habitat and agricultural land cover mapping’, *ISPRS Journal of Photogrammetry and Remote Sensing*. DOI: 10.1016/j.isprsjprs.2007.03.003

Mitchell, A. L., Rosenqvist, A., & Mora, B. (2017). ‘Current remote sensing approaches to monitoring forest degradation in support of countries measurement, reporting and verification (MRV) systems for REDD+’. *Carbon Balance and Management*. DOI: 10.1186/s13021-017-0078-9

MOEF. (2018). *REPUBLIC OF KENYA MINISTRY OF ENVIRONMENT AND FORESTRY Taskforce Report on Forest Resources Management and Logging Activities in Kenya*. Retrieved from <http://www.environment.go.ke/wp-content/uploads/2018/08/Forest-Report.pdf>

MOEF (Ministry of Environment and Forestry). (2018). *Economic Value of the Water Towers in Kenya*. Retrieved from <https://www.kefri.org/PDF/Publications/ESV Summary acg nms.pdf>

MOEWNR, (Ministry of Environment Water and Natural Resources). (2014). ‘Forest policy in

Kenya', *Nature*, 180/4587: 22. DOI: 10.1038/180636d0

Njoka, J. T., Yanda, P., Maganga, F., Liwenga, E., Kateka, A., Henku, A., Mabhuye, E., et al. (2016). 'Kenya: Country Situation Assessment', *Research for Climate-resilient Future*.

Nunes, A., & Caetano, M. (2006). 'Forest monitoring with remote sensing: A web application for the common user'. *American Society for Photogrammetry and Remote Sensing - Annual Conference of the American Society for Photogrammetry and Remote Sensing 2006: Prospecting for Geospatial Information Integration*.

Omondi, L., & Musula, P. (2011). 'Land Degradation of the Mau Forest Complex in Eastern Africa: A Review for Management and Restoration Planning'. *Environmental Monitoring*. DOI: 10.5772/28532

Ongugo, P. O., Langat, D., Oeba, V. O., Kimondo, J. M., Owuor, B., Njuguna, J., Okwaro, G., et al. (2014). *WORKING PAPER A review of Kenya ' s national policies relevant to climate change adaptation and mitigation Insights from Mount Elgon* (No. Working paper 155).

Penman, J., Gytarsky, M., Hiraishi, T., Krug, T., Kruger, D., Pipatti, R., Buendia, L., et al. (2003). *Good Practice Guidance for Land Use, Land-Use Change and Forestry*. *IPCC*.

Potapov, P. V., Dempewolf, J., Talero, Y., Hansen, M. C., Stehman, S. V., Vargas, C., Rojas, E. J., et al. (2014). 'National satellite-based humid tropical forest change assessment in Peru in support of REDD+ implementation', *Environmental Research Letters*. DOI: 10.1088/1748-9326/9/12/124012

Potapov, Peter V., Turubanova, S. A., Hansen, M. C., Adusei, B., Broich, M., Altstatt, A., Mane, L., et al. (2012). 'Quantifying forest cover loss in Democratic Republic of the Congo, 2000-2010, with Landsat ETM+ data', *Remote Sensing of Environment*. DOI: 10.1016/j.rse.2011.08.027

Rodriguez-Galiano, V. F., Ghimire, B., Rogan, J., Chica-Olmo, M., & Rigol-Sanchez, J. P. (2012). 'An assessment of the effectiveness of a random forest classifier for land-cover classification', *ISPRS Journal of Photogrammetry and Remote Sensing*. DOI: 10.1016/j.isprsjprs.2011.11.002

Serra, P., Pons, X., & Saurí, D. (2003). 'Post-classification change detection with data from different sensors: Some accuracy considerations', *International Journal of Remote Sensing*. DOI: 10.1080/0143116021000021189

Soini, E. (2007). 'Land tenure and land management in the districts around Mount Elgon: An assessment presented to Mount Elgon Regional Ecosystem Conservation Programme (MERECP)', 59.

Stednick, J. D. (1996). 'Monitoring the effects of timber harvest on annual water yield', *Journal of Hydrology*. DOI: 10.1016/0022-1694(95)02780-7

Steffen, W., Richardson, K., Rockström, J., Cornell, S. E., Fetzer, I., Bennett, E. M., Biggs, R., et al. (2015). 'Planetary boundaries: Guiding human development on a changing planet', *Science*. DOI: 10.1126/science.1259855

Strahler, A. H., Boschetti, L., Foody, G. M., Friedl, M. a., Hansen, M. C., Herold, M., Mayaux, P., et al. (2006). 'Global Land Cover Validation: Recommendations for Evaluation and Accuracy Assessment of Global Land Cover Maps', *Change*. DOI: 10.1080/01431160512331326521

Syktus, J. I., & McAlpine, C. A. (2016). 'More than carbon sequestration: Biophysical climate benefits of restored savanna woodlands', *Scientific Reports*. DOI: 10.1038/srep29194

The World Summit on Sustainable Development. (2005). *The World Summit on Sustainable Development*. DOI: 10.1007/1-4020-3653-1

UN. (2014). 'International Decade for Action "Water for Life" 2005-2015. Focus Areas: The human right to water and sanitation'. *United Nations*.

UNCCD. (2014). *Desertification: The Invisible Frontline*. *United Nations Convention to Combat Desertification*.

'United Nations Convention on Biological Diversity.',. (1996). *Journal of ethnopharmacology*. DOI: 10.4324/9780429273964-8

Viviroli, D., Dürr, H. H., Messerli, B., Meybeck, M., & Weingartner, R. (2007). 'Mountains of the world, water towers for humanity: Typology, mapping, and global significance', *Water Resources Research*. DOI: 10.1029/2006WR005653

Wallström, M., Bolin, B., Crutzen, P., & Steffen, W. (2004). 'A global crisis: The Earth's life-support system in peril'. *International Herald tribune*.

Werth, D., & Avissar, R. (2005). 'The local and global effects of African deforestration', *Geophysical Research Letters*. DOI: 10.1029/2005GL022969

Wiegandt, E. (2017). 'Mountains: Sources of Water, Sources of Knowledge', *GAIA - Ecological Perspectives for Science and Society*. DOI: 10.14512/gaia.11.3.1

Williams, C. A., Reichstein, M., Buchmann, N., Baldocchi, D., Beer, C., Schwalm, C., Wohlfahrt, G., et al. (2012). ‘Climate and vegetation controls on the surface water balance: Synthesis of evapotranspiration measured across a global network of flux towers’, *Water Resources Research*. DOI: 10.1029/2011WR011586

Zarembka, D. (n.d.). ‘#569 — A Problem with Reforestation in Kenya – Reports from Kenya’. Retrieved February 8, 2020, from <http://davidzarembka.com/2019/09/26/569-a-problem-with-reforestation-in-kenya/>

Zhang, S., Yang, H., Yang, D., & Jayawardena, A. W. (2016). ‘Quantifying the effect of vegetation change on the regional water balance within the Budyko framework’, *Geophysical Research Letters*. DOI: 10.1002/2015GL066952

APPENDIX I: IMAGE ACQUSITION SCRIPT (Google Earth Engine)

```
/////////////////////////////////////////////////////////////////////////////
//////////
// Code to generate country wide mosaics using Landsat 5, 7 and 8 surface
reflectance
// http://www.conservation.org/about/gef/Pages/NDVI.aspx
// by Mariano Gonzalez-Roglich (mgonzalez-roglich@conservation.org)
//Customized by Kuto Edmond (edmondkuto0@gmail.com)
/////////////////////////////////////////////////////////////////////////////
//////////

// User inputs
var sa_name = "KE"; // ISO code of the country
var year_str = 2019;
var year_end = 2019;
var day_str = 0; // starting day for the period used to produce mosaic (0 =
january 1st)
var day_end = 364; // ending day for the period used to produce the mosaic
(364 = december 31st)

// End of user inputs

/////////////////////////////////////////////////////////////////////////////
///
// Define country outline based on name
var sa = ee.FeatureCollection("users/Kuto/Major_towers");

var buffer = function(feature) {
  return feature.buffer(10000,1000);};

var sa_buf = sa.map(buffer);

Map.addLayer(sa_buf);

// Definition of season start and end dates.
var startDate = ee.Date.fromYMD(year_str,1,1).advance(day_str,'day');
var endDate = ee.Date.fromYMD(year_end,1,1).advance(day_end,'day');
print('Start and end dates:',startDate,endDate);

// Function to mask clouds
var cloud_masking = function(in_sr) {
  // Use the fmask provided
  var mask = in_sr.select('pixel_qa').bitwiseAnd(2).neq(0);
  var masked = in_sr.updateMask(mask);
  return masked;
};

// Subset of bands to use for mosaics
var sensorBandDictLandsatSR =ee.Dictionary({L8 : ee.List([1,2,3,4,5,6,10]),
                                            L7 : ee.List([0,1,2,3,4,6,9]),
                                            L5 : ee.List([0,1,2,3,4,6,9])});
var bandNamesLandsatSR =
ee.List(['blue','green','red','nir','swir1','swir2','pixel_qa']);

//Acquire Landat
```

```
var l5SRs = ee.ImageCollection('LANDSAT/LT05/C01/T1_SR')
    .filterDate(startDate,endDate)
    .filter(ee.Filter.calendarRange(day_str,day_end))
    .filterBounds(sa_buf)
    .select(sensorBandDictLandsatSR.get('L5'),bandNamesLandsatSR);
var l7SRs = ee.ImageCollection('LANDSAT/LE07/C01/T1_SR')
    .filterDate(startDate,endDate)
    .filter(ee.Filter.calendarRange(day_str,day_end))
    .filterBounds(sa_buf)
    .select(sensorBandDictLandsatSR.get('L7'),bandNamesLandsatSR);
var l8SRs = ee.ImageCollection('LANDSAT/LC08/C01/T1_SR')
    .filterDate(startDate,endDate)
    .filter(ee.Filter.calendarRange(day_str,day_end))
    .filterBounds(sa_buf)
    .select(sensorBandDictLandsatSR.get('L8'),bandNamesLandsatSR);

// Print number of available image per collection.
print(l5SRs);
print(l7SRs);
print(l8SRs);

// If startDate is before 2013 it will use all the images available from L5 &
7
// If startDate is after  2013 it will use images from L8 to generate the
main mosaic,
//    and use a L7 mosaic to fill gaps with no data (this is done to minimize
L7 stripping).
if (year_str < 2013){
  var ls = ee.ImageCollection(l5SRs.merge(l7SRs));
  var m_ls = ls.map(cloud_masking);
  var mosaic =
m_ls.select('blue','green','red','nir','swir1','swir2').reduce('median').int3
2();}
  //var mosaic_v =
m_ls.select('blue','green','red','nir','swir1','swir2').reduce('variance').in
t32();
  //var mosaic = ee.Image.cat([mosaic_m, mosaic_v]);}
else{
  var m_l8SRs = l8SRs.map(cloud_masking);
  var mosaic8_m =
m_l8SRs.select('blue','green','red','nir','swir1','swir2').reduce('median').i
nt32();
  //var mosaic8_v =
m_l8SRs.select('blue','green','red','nir','swir1','swir2').reduce('variance')
.clipToCollection(sa_buf).int32();
  var m_l7SRs = l7SRs.map(cloud_masking);
  var mosaic7_m =
m_l7SRs.select('blue','green','red','nir','swir1','swir2').reduce('median').i
nt32();
  //var mosaic7_v =
m_l7SRs.select('blue','green','red','nir','swir1','swir2').reduce('variance')
.int32();
  var mos_coll_m = ee.ImageCollection([mosaic7_m,mosaic8_m]);
  //var mos_coll_v = ee.ImageCollection([mosaic7_v,mosaic8_v]);
  var mosaic = mos_coll_m.mosaic();}
  //var mosaic_v = mos_coll_v.mosaic()
  //var mosaic = ee.Image.cat([mosaic_m, mosaic_v]);}
```

```
var mosaic = mosaic.clipToCollection(sa_buf).select(

['blue_median','green_median','red_median','nir_median','swir1_median','swir2
_median'], // old names
    ['blue','green','red','nir','swir1','swir2']                // new names
);


// // Center display to country extent
// Map.centerObject(sa);
// // Display final mosaic
Map.addLayer(mosaic, {'min': 0,'max': 4000,   'bands':'red,green,blue'},
'mosaic_real');
Map.addLayer(mosaic, {'min': 0,'max': 4000,   'bands':'nir,red,green'},
'mosaic_false');


Export.image.toDrive({
image: mosaic,
description: 'Towers_2019',
maxPixels: 10000000000000,
scale: 30,
region: sa_buf.geometry().bounds(),
});
```

APPENDIX II: IMAGE CLASSIFICATION SCRIPT (RStudio)

```
############################################################################
# This script was written by Ned Horning [horning@amnh.org]
# Support for writing and maintaining this script comes from The John D. and
# Catherine T. MacArthur Foundation and Google.org.
#
# This script is free software; you can redistribute it and/or modify it
under the
# Terms of the GNU General Public License as published by the Free Software
Foundation either version 2 of the License, or (at your option) any later
version.                                *
#
#This script was customized by Kuto Edmond (edmondkut0@gmail.com)
############################################################################
#Load libraries
require(maptools)
require(sp)
require(randomForest)
require(raster)
require (rgdal)
#
cat("Set variables and start processing\n")
#
############################   SET VARIABLES HERE
###################################
# Set working directory
setwd("X:\\MScGIS 2018\\Thesis\\Images\\Major_towers")
# Name and path for the Shapefile (don't need the .shp extension)
shapefile <- '2010_training.shp'
# Class numbers that you want to select training sample from
classNums <- c(1,2)
# For each land cover class the approximate number of training samples to be
randomly selected
# If a value is "0" then all pixels in all of the polygons for that class
will be used
classSampNums <- c(1000, 1000)
# Name of the attribute that holds the integer land cover type identifier
attName <- 'LC_Code'
# No-data value for the input image
nd <- 0
# Name and path for the input satellite image
inImageName <-'Towers_2010_clip.tif'
# Name and location of the output Shapefile point file that will be created.
If this output
# is not needed you can enter two double or single-quotes (""?? or '')
# Note that if this file exists the write will fail with the message
"Creation of output file failed"
outMarginFile <- 'margin.shp'
# Output classification image (enter TRUE or FALSE)
classImage <- TRUE
# Output probability image layer (enter TRUE or FALSE)
probImage <- TRUE
# Output classification layer and set pixels with probability less than
"probThreshold" to 0 (enter TRUE or FALSE)
threshImage <- TRUE
```

```
# Enter threshold probability in percent (values must be between 0 and 100)
only used if threshImage=TRUE
probThreshold <- 75
# Layer number (band number) for the X and Y axis of the feature space plot.
# If you do not want to calculate a feature plot enter 0 as the layer number
xBand <- 0
yBand <- 4
###############################################################################
##########
#
# Start processing
startTime <- Sys.time()
cat("Start time", format(startTime),"\n")

# Read the Shapefile
shapefileLayerName <- strsplit(tail(unlist(strsplit(shapefile, "/")), n=1),
"\\.")[[1]] [1]
vec <- readOGR(shapefile, shapefileLayerName)

# Load the image then flag all no-data values(nd) so they are not processed
satImage <- brick(inImageName)
NAvalue(satImage) <- nd
#for (b in 1:nlayers(satImage)) { NAvalue(satImage@layers[[b]]) <- nd }

# Create vector of unique land cover attribute values
allAtt <- vec@data
tabAtt <-table(allAtt[[attName]])
uniqueAtt <-as.numeric(names(tabAtt))

# Check if lenght of classNums and classSampNums is equal
if (length(classNums) != length(classSampNums)) {
  cat("\n**************length of classNums and classSampNums no
equal**************** \n")
  stop("Check the classNums and classSampNums variable\n", call.=FALSE)
}

# Check if all classNums exist in uniqueAtt
#### CHECK THIS FUNCTION TO SEE IF classNums ARE IN uniqueAtt
################
if (sum(classNums %in% uniqueAtt) != length(uniqueAtt)) {
  cat("\n*******not all classes in classNums are defined in the vecotr
file******* \n")
  stop("Check classNums and vector attribute table\n", call.=FALSE)
}

# Create input data from a Shapefile using all training data
cat("Create training data using all pixels in training polygons\n")
predictors <- data.frame()
response <- numeric()
xyCoords <- data.frame()

cat("Create training data to train model\n")
# If all pixels in a polygon are to be used process this block
for (n in 1:length(classNums)) {
  if (classSampNums[n] == 0) {
    # Get the metadata for all polygons for this particular class
    class_data<- vec[vec[[attName]]==classNums[n],]
```

```
    # Extract and combine predictor and response variables for each polygon
within a class
    for (i in 1:dim(class_data)[1]) {
      satValues <- extract(satImage, class_data[i,], cellnumbers=TRUE,
df=TRUE)
      ## satValues <- as.data.frame(do.call(rbind,satValues))
      attributeVector <- rep.int(classNums[n],nrow(satValues))
      xyCoords <- rbind(xyCoords, xyFromCell(satImage, satValues[,2]))
      predictors <- rbind(predictors, satValues[,-1:-2])
      response <- c(response, attributeVector)

    }
  } else {
    # Create input data from a Shapefile by sampling training data polygons
    # Get the metadata for all polygons for a particular class (based on the
uniqueAtt variable)
    class_data<- vec[vec[[attName]]==classNums[n],]
    # Get the area of each polygon for a particular class
    areas <- sapply(slot(class_data, "polygons"), slot, "area")
    # Calculate the number of samples for each polygon based on the area in
proportion to total area for a class
    nsamps <- ceiling(classSampNums[n]*(areas/sum(areas)))
    # Use random sampling to select training points (proportial based on
area) from each polygon for a given class
    for (i in 1:dim(class_data)[1]) {
      xy_class <- spsample(class_data[i,], type="random", n=nsamps[i])
      # Add coordinates to create a list of random points for all polygons
      if (i == 1) cpts <- xy_class
      else cpts <- rbind(cpts, xy_class)
    }
    # The number of points might not match numsamps exactly.
    xy_ForClass <- cpts
    xyCoords <- rbind(xyCoords, xy_ForClass@coords)

    # Get class number for each sample point for responce variable
    response <- c(response, over(xy_ForClass, vec)[[attName]])
    # Get pixel DNs from the image for each sample point
    predictors <- rbind(predictors, extract(satImage, xy_ForClass))
  }
}

trainvals <- cbind(response, predictors)

# Test if feature space plot is needed
if (xBand != 0 & yBand != 0) {
  #Plot feature space and samples
  continue <- "c"
  while (continue == "c") {
    plotImage <- stack(satImage[[xBand]], satImage[[yBand]])
    # Get pixel values from the image under each sample point and create a
table with
    # observed and predicted values
    cat("Getting pixel values to create feature space plot\n\n")
    featurePlotPoints <- sampleRegular(plotImage,100000 )

    # Remove NA values from trainvals table created above
    featurePlotPoints <- na.omit(featurePlotPoints)
```

```
    minBand1 <- min(featurePlotPoints[,1])
    maxBand1 <- max(featurePlotPoints[,1])
    minBand2 <- min(featurePlotPoints[,2])
    maxBand2 <- max(featurePlotPoints[,2])
    rangeBand1 <- maxBand1 - minBand1 + 1
    rangeBand2 <- maxBand2 - minBand2 + 1

    xAxisLabel <- paste("Layer", xBand, sep=" ")
    yAxisLabel <- paste("Layer", yBand, sep=" ")

    plot(featurePlotPoints[,1], featurePlotPoints[,2], col="lightgrey",
xlab=xAxisLabel, ylab=yAxisLabel)

    uniqueValues <- unique(trainvals[,1])
    for (v in 1:length(uniqueValues)) {
      points(trainvals[which(trainvals[,1]==uniqueValues[v]), xBand+1],
trainvals[which(trainvals[,1]==uniqueValues[v]), yBand+1], col=v, pch=20)
    }

    legend(minBand1, maxBand2, col=1:v, pch=20, title="Classes",
legend=as.character(uniqueValues))

    continue <- readline(prompt="Type n to stop, c to change feature space
bands, s to define a rectangle to locate gaps in feature space, or any other
key to continue with randome forests model creation and prediciton: \n\n")

    if (substr(continue, 1,1) == "n") {
      stop("Processing stopped at users request \n\n", call.=FALSE)
    }
    if (substr(continue, 1,1) == "s") {
      cat("Click two points to define the area on the feature space plot that
you want to highlight\n")
      coords <- locator(n=2)
      coords <- unlist(coords)
      xvals <- coords[1:2]
      yvals <- coords[3:4]

      # Print out the corner coordinates for the rectangle
      cat("min X =", min(xvals), "\n")
      cat("max X =", max(xvals), "\n")
      cat("min y =", min(yvals), "\n")
      cat("max y =", max(yvals), "\n")

      # Draw the rectangle on the feature space plot
      rectangle <- matrix(nrow=5, ncol=2)
      rectangle[1,] <- c(min(xvals), max(yvals))
      rectangle[2,] <- c(max(xvals), max(yvals))
      rectangle[3,] <- c(max(xvals), min(yvals))
      rectangle[4,] <- c(min(xvals), min(yvals))
      rectangle[5,] <- c(min(xvals), max(yvals))
      lines(rectangle[,1], rectangle[,2])

      # Get the bands used to calculate the feature space plot
      b1 <- raster(plotImage, layer=1)
      b2 <- raster(plotImage, layer=2)
```

```
      # Threshold satImage so all values selected in the rectangle on the
feature space plot are set to 255
      satImage[(b1 > min(xvals)) & (b1 < max(xvals)) & (b2 > min(yvals)) &
(b2 < max(yvals))] <- 255

      # Plot the thresholded image with selected pixels displayed as white
pixels
      plotRGB(satImage, r=1,g=2,b=3, , stretch='hist')
      cat("White pixels in the plotted image were selected in the rectangle
drawn on the feature space plot")
      stop("Add new training data and re-run the script \n\n", call.=FALSE)
    }
    if (substr(continue, 1,1) == "c") {
      xBand <- as.numeric(readline(prompt="Enter the band number for the x
axis: \n"))
      yBand <- as.numeric(readline(prompt="Enter the band number for the y
axis: \n"))
    }
  }
}

# Remove NA values
trainvals <- na.omit(trainvals)

# Check to make sure Shapefile and input image are in the same projection
if (nrow(trainvals) == 0) {
  cat("\n*************************No training data
found***************************** \n")
  stop("It is possible the projection of the Shapefile with training data and
input image are different\nCheck projections and run again", call.=FALSE)
}

# Run Random Forest
cat("Calculating random forest object\n")
randfor <- randomForest(as.factor(response) ~., data=trainvals,
importance=TRUE, na.action=na.omit)

# Start predictions
cat("Starting predictions\n")
# Calculate the image block size for processing
bs <- blockSize(satImage)

extensionName <- unlist(strsplit(inImageName,
"\\."))[length(unlist(strsplit(inImageName, "\\.")))]
outFileBaseName <- unlist(strsplit(inImageName, paste("\\.", extensionName,
sep="")))[1]

# Create the output rasters
if (classImage) {
  outClassImage <- raster(satImage)
  outClassImage <- writeStart(outClassImage, filename=paste(outFileBaseName,
"_Class.tif", sep=""), navalue=0, progress='text', format='GTiff',
datatype='INT1U', overwrite=TRUE)
}
if (probImage) {
  outProbImage <- raster(satImage)
  outProbImage <- writeStart(outProbImage, filename=paste(outFileBaseName,
```

```
"_Prob.tif", sep=""), navalue=0, progress='text', format='GTiff',
datatype='INT1U', overwrite=TRUE)
}
if (threshImage) {
  outThreshImage <- raster(satImage)
  outThreshImage <- writeStart(outThreshImage,
filename=paste(outFileBaseName, "_Thresh.tif", sep=""), navalue=0,
progress='text', format='GTiff', datatype='INT1U', overwrite=TRUE)
}

# Loop though each of the image blocks to calculate the output layers
selected in the variables section
for (i in 1:bs$n) {
  cat("processing block", i, "of", bs$n, "\r")
  imageBlock <-  getValuesBlock(satImage, row=bs$row[i], nrows=bs$nrows[i])
  predValues <- predict(randfor, imageBlock, type='response')
  classValues <- as.numeric(levels(predValues))[predValues]

  if (classImage) {
    #outClassMatrix <- matrix(classValues, nrow=nrow(imageBlock), ncol=1)
    outClassImage <- writeValues(outClassImage, classValues, bs$row[i])
  }
  if (probImage || threshImage) {
    predProbs <- as.data.frame(predict(randfor, imageBlock, type='prob'))
    maxProb <- round(apply(predProbs, 1, max) * 100)
    if (probImage) {
      #outProbMatrix <- matrix(maxProb, nrow=nrow(imageBlock), ncol=1)
      outProbImage <- writeValues(outProbImage, maxProb, bs$row[i])
    }
    if (threshImage) {
      threshValues <- classValues
      threshValues[which(maxProb <= probThreshold)] <- 0
      #outThreshMatrix <- matrix(threshValues, nrow=nrow(imageBlock), ncol=1)
      outThreshImage <- writeValues(outThreshImage, threshValues, bs$row[i])
    }
  }
}

# Stop writing and close the file
if (classImage) {
  outClassImage <- writeStop(outClassImage)
}
if (probImage) {
  outProbImage <- writeStop(outProbImage)
}
if (threshImage) {
  outThreshImage <- writeStop(outThreshImage)
}

# Print error rate and confusion matrix for this classification
confMatrix <- randfor$confusion
cat("#########################################################################
#########\n")
cat("OOB error rate estimate\n", 1 - (sum(diag(confMatrix)) /
sum(confMatrix[,1:ncol(confMatrix)-1])), "%\n\n", sep="")
cat("Confusion matrix\n")
print(randfor$confusion)
```

```r
cat("\n")

if (outMarginFile != "") {
  # Calculate margin (proportion of votes for correct class minus maximum
proportion of votes for other classes)
  marginData <- margin(randfor)
  trainingAccuracy <- cbind(marginData[order(marginData)],
trainvals[order(marginData),1])

  # Add column names to attributes table
  colnames(trainingAccuracy) <- c("margin", "classNum")
  # Order X and Y coordinates
  xyCoords <- xyCoords[order(marginData),]

  # Create and write point Shapefile with margin information to help improve
training data
  row.names(trainingAccuracy) <- NULL
  pointVector <- SpatialPointsDataFrame(xyCoords,
as.data.frame(trainingAccuracy), proj4string = satImage@crs, match.ID =
FALSE)
  writeOGR(pointVector, outMarginFile, "layer", driver="ESRI Shapefile",
check_exists=TRUE)
}

# Plotting variable importance plot
varImpPlot(randfor)

# Calculate processing time
timeDiff <- Sys.time() - startTime
cat("\nProcessing time", format(timeDiff), "\n")
```